First of all, we would like to thank reviewers for their valuable comments on our manuscript. We revised our manuscript carefully by taking these comments into account.

General comments

This paper describes results from a single cruise conducted in the autumn of 2013. The hydrography in the region investigated is complex and with large seasonal signatures. The analysis of water types from salinity and alkalinity provides a convincing picture of the distribution of water from different sources and is thus a key to the interpretation of the surface and water column data on dissolved oxygen and carbon dioxide. The primary result reported, as seen from the title of this communication, is a low subsurface pCO2 and negative AOU in the Canada Basin. The authors suggest that this feature, a hidden CO2 sink formed previously in the year, may have significance in the changing Arctic Ocean. Two figures are used to demonstrate this feature, numbers 5 and 6. Strangely, there are much more pCO2 data points for Canada Basin Water in Fig. 6 than in Fig 5e. Fig. 6 indicates a qualitative relation between pCO2 and AOU. This reviewer finds it necessary that to make the paper acceptable for publication, the authors explore these relations deeper and quantitatively in order to underpin the roles of photosynthesis, respiration and mixing. Also to examine the likely influence of time from formation to observation.

Data have been shown for the entire water column in the Canada Basin in Figure 6a but only for top 60 m in Figure 5e. In Figure 5 in the revised manuscript, we show the data down to the depth of 180 m according to comments by reviewer #2. Figure 6c and 6d were added for quantitative discussion on the subsurface low $p\mathrm{CO}_2$. There were two boundaries in preformed DIC_{33} and nutrients around $S = 29.3$ and $S = 33.1$. Former and latter corresponded with temperature minimum of rWML and PWW respectively. The layer above $S = 29.3$ was formed in the Chukchi Sea. Water between $S = 29.3$ and $S = 33.1$ can be divided into PSW and PWW by temperature maxiumum around $S = 31$. These were formed in the Chukchi Sea and subducted to the Canada Basin. Low $p\mathrm{CO}_2$ was limited in the upper portion of Pacific origin water, i.e., PSW. This was because DIC in PSW was originally lower, and biological production further reduced it.

Specific comments

Page Line

3 1 Add information on where cruise started and refer to Fig. 3.

The research cruise departed from Dutch Harbor, Alaska on August 31st 2013. This paper focused only a portion of the cruise. This was because general variations in surface $p\mathrm{CO}_2^{\mathrm{sea}}$ in the Western Arctic Ocean have already been well investigated (Bates 2006, Cai et al., 2010). The results from this cruise were not much different from these reports. Therefore, we highlighted water mass characteristic and CO_2 dynamics in the subsurface. Information on the overall cruise and the reason why we presented the results from a part of the cruise were added to the revised manuscript.

3 8 Is the instrument calibration response linear? What is the estimated uncertainty of measurements reported significantly outside the calibration range?

Response of CRDS we used to the change in the CO_2 concentration is practically linear. When we used three standard gases ranging from 206.34 ppmv to 489.28 ppmv for calibration, the residual of each data from linear regression was less than 0.03 ppmv. According to the manufacturer, precision of CO_2 measurement above 500 ppmv is 0.1%.

3 9 Add reference to the "WMO scale“.

Zhao and Tans (2006) was added as the reference. “WMO scale” was replaced by “WMO X2007 scale” to eliminate ambiguity.

3 16 Name of author is here Midorikawa but Mirorikawa in the list of references.

“Mirorikawa” was changed to “Midorikawa” according to the reviewer’s comment.

3 26 Were the DIC bottles closed after filling?

The bottles were always capped with a screw type lid. Bottle filling, transport to measurement system, and discharge were all done through high-density PFA-tubes mounted through the lid.

3 28 The reference (Nippon ANS, Japan) is unsufficient for a description of the instrumentation of extraction/coulometric titration system.

The system was comprised of seawater dispensing unit, a CO_2 extraction unit, and a coulometer (Model 3000, Nippon ANS, Inc.). The dispensing unit dispenses the seawater from a glass bottle to a pipette of nominal 15 ml volume. The pipette was kept at 20 ± 0.05 °C by a water jacket. Dissolved CO_2 in seawater was extracted in a stripping chamber of the CO_2 extraction unit by adding 2 cm^3 of phosphoric acid (10% v/v). Extracted CO_2 was transferred to the coulometer by pure nitrogen gas. Information about the system was added to the revised manuscript.

4 4 To which depth were water samples collected?

Depths of the sample collections in the top 200 m were 0, 5, 10, 20, 30, 40, 50, 75, 100, 125, 150 and 200 m. Samples were also collected at the surface chlorophyll maximum that ranged from 12 m to 92 m. This information was added to the revised manuscript.

4 8 Change "same physical conditions“ to "same potential temperature and salinity conditions“.

“physical conditions” was changed to “potential temperature and salinity conditions” according to the comment.

4 10 How were the chlorophyll measurements calibrated?

The instrument was calibrated against pure chlorophyll-a (Sigma-Aldrich Co. LLC.). Description about the calibration was added to the revised manuscript.

4 14 The reference (Nippon ANS, Japan) is unsufficient for a description of the instrumentation used for TA measurements.

Measurement of alkalinity was made using a spectrophotometric system (Nippon ANS, Inc.) based on the scheme of Yao and Byrne (1998). The seawater sampled in the glass bottle is transferred to a sample cell via dispensing unit. The length and volume of the cell are 8 cm and 13 cm^3, respectively, and its temperature is kept at 25°C. The TA is calculated by measuring two sets of absorbance at three wavelengths (750, 616 and 444 nm). One is the absorbance of seawater sample before injecting an acid with indicator solution (bromocresol green) and another is the one after the injection of the solution and mixing for 8.5 minutes. Information about system was added to the revised manuscript.

4 18 Which computation package is used to compute ocean carbonate chemistry?

We used for macro package of CO2SYS program for Microsoft Excel (Pierrot et al., 2006). Usage and reference were added.

5 7 Change TARRO to TArro

"TARRO" was changed to "TA_{RRO}" according to the reviewer's comment.

6 5 Analysis of satellite imaginary is not mentioned in the Data and Methods section. Which data and how processed needs to be added.

NPP estimation was based on Vertiacal Generalized Production Model by Behrenfeld and Falkowski, (1997). In this method, NPP is estimated from empirical equations. Chlorophyll, sea surface temperature and photosynthetically active radiation obtained by satellite are used as variables. Length of the daytime is also used for the calculation. Description and reference was added to "Measurements and data" section.

6 9 The calculation of CO2 flux and quantification of $\Delta p\mathrm{CO}_2$ reduction needs more detail.

At first, initial condition of temperature, salinity, DIC, TA and mixed layer depth was set.

Initial $p\mathrm{CO}_2$ ($p\mathrm{CO}_2{}^0$) was calculated. Initial $\Delta p\mathrm{CO}_2$ ($\Delta p\mathrm{CO}_2{}^0$) was the difference between $p\mathrm{CO}_2{}^0$ and atmospheric $p\mathrm{CO}_2$ ($p\mathrm{CO}_2{}^{air}$).

$$pCO_2{}^0 = f(T, S, DIC, TA)$$

$$\Delta pCO_2^0 = pCO_2^0 - \ pCO_2^{air}$$

All parameter except DIC were fixed during the calculation, i.e. evaporation, precipitation and lateral/vertical advection were assumed unchanged. Flux of CO_2 (F_{CO2}) was calculated from wind speed and gas transfer coefficient. Time step was set to one day. Here, k and K_0 denote the solubility of CO_2 by Weiss (1974) and gas transfer coefficient by Wanninkhof (2014) respectively.

$$F_{CO2} = \ kK_0\Delta pCO_2$$

$$k = 0.251 \ \cdot U_{10}^2 \cdot (Sc/660)^{-0.5}$$

Increase in DIC in each time step was calculated from F_{CO2}.

$$\Delta \mathrm{DIC} = \frac{F_{CO2}}{MLD * \ \rho(T,\ S)}$$

$$DIC_{t+1} = DIC_t + \ \Delta DIC$$

Here, MLD and $\rho(T, S)$ mean mixed layer depth [m] and density of seawater in mixed layer [kg m^{-3}] respectively. After each time step, pCO_2^t and ΔpCO_2^t were calculated from DIC at the time.

$$pCO_{2,t} = f(T, S, DIC_t, TA)$$

$$\Delta pCO_2^t = pCO_2^t - \ pCO_2^{air}$$

Half-life means the time required to reduceΔpCO_2^t to half of ΔpCO_2^0. Description of these processes for calculation of half-life was added to “Calculation” section.

6 20 Change "High“ to "Near equilibrium“conditions.

“High” was changed to “Near equilibrium” according to the reviewer’s comment.

7 10 At what depth lies the NSTM?

Temperature maximum around S = 28.8 in Figure 4c was deemed as NSTM. The depths of NSTM ranged between 15 and 26 m.

7 19 Suggest changing "affected“ to "contributed to“.

“affected” will be changed to “contributed to” according to the reviewer’s comment.

7 31 A figure is needed to illustrate the distinctiveness of the CBW subsurface minima.

Figure 6c and 6d indicated that PSW had lower preformed DIC than surface water and that significant amounts of nutrients remained in PSW. Low pCO_2 in PSW was attributable to low preformed DIC and biological production.

14 Fig. 1 The placement of this figure as Fig. 1 is strange. It should be after Data and Methods.

15 Fig. 2 The placement of this figure as Fig. 2 is strange. It should be after Data and Methods.

We divided “Data and Methods” into two new sections, “Measurements and Data” and

“Calculations”. These two figures and related descriptions were moved to “Calculations” section.

19 Fig.5 Using the calendar date of data collection on the x-axis is unusual. Particularly as there is no date information with the cruise tracks in Fig. 3. Is it possible to use distance sailed instead?
X-axis of Figure 5 was changed to the distance from the start of cruise. Please see Figure 5 (revised) attached.

20 Fig. 5f The colour scale does not include the blue observed at lower depths.
Color scale changed to cover wider range including positive AOU. Triangles on the color bar were enlarged.

Reference

Bates, N. R. (2006), Air-sea CO_2 fluxes and the continental shelf pump of carbon in the Chukchi Sea adjacent to the Arctic Ocean, J. Geophys. Res., 111, C10013, doi:10.1029/2005JC003083.

Behrenfeld, M. J. and Falkowski, P. G., (1997), A consumers guide to phytoplankton primary production models, Limnol. Oceanogr., 42(7), 1479–1491.

Cai, W.-J., Chen, L., Chen, B., Gao, Z., Lee, S.H., Chen, J., Pierrot, D., Sullivan, K., Wang, Y., Hu, X., Huang, W.-J., Zhang, Y., Xu, S., Murata, A., Grebmeier, J. M., Jones, E. P., and Zhang, H. (2010), Decrease in the CO_2 uptake capacity in an ice-free Arctic Ocean basin, Science, 329, 556–559, doi:10.1126/science.1189338.

Pierrot, D. E. Lewis, and D. W. R. Wallace. (2006), MS Excel Program Developed for CO_2 System Calculations, ORNL/CDIAC-105a. Carbon Dioxide Information Analysis Center, Oak Ridge National Laboratory, U.S. Department of Energy, Oak Ridge, Tennessee. doi: 10.3334/CDIAC/otg.CO2SYS_XLS_CDIAC105a

Yao, W. S. and Byrne, R. H, (1998), Simplified seawater alkalinity analysis: Use of linear array spectrometers, Deep Sea Res., PartI, 45(8), 1383–1392, doi:10.1016/S0967-0637(98)00018-1.

Zhao, C. L., and P. P. Tans, (2006), Estimating uncertainty of the WMO mole fraction scale for carbon dioxide in air, J. Geophys. Res., 111, D08S09, doi:10.1029/2005JD006003.

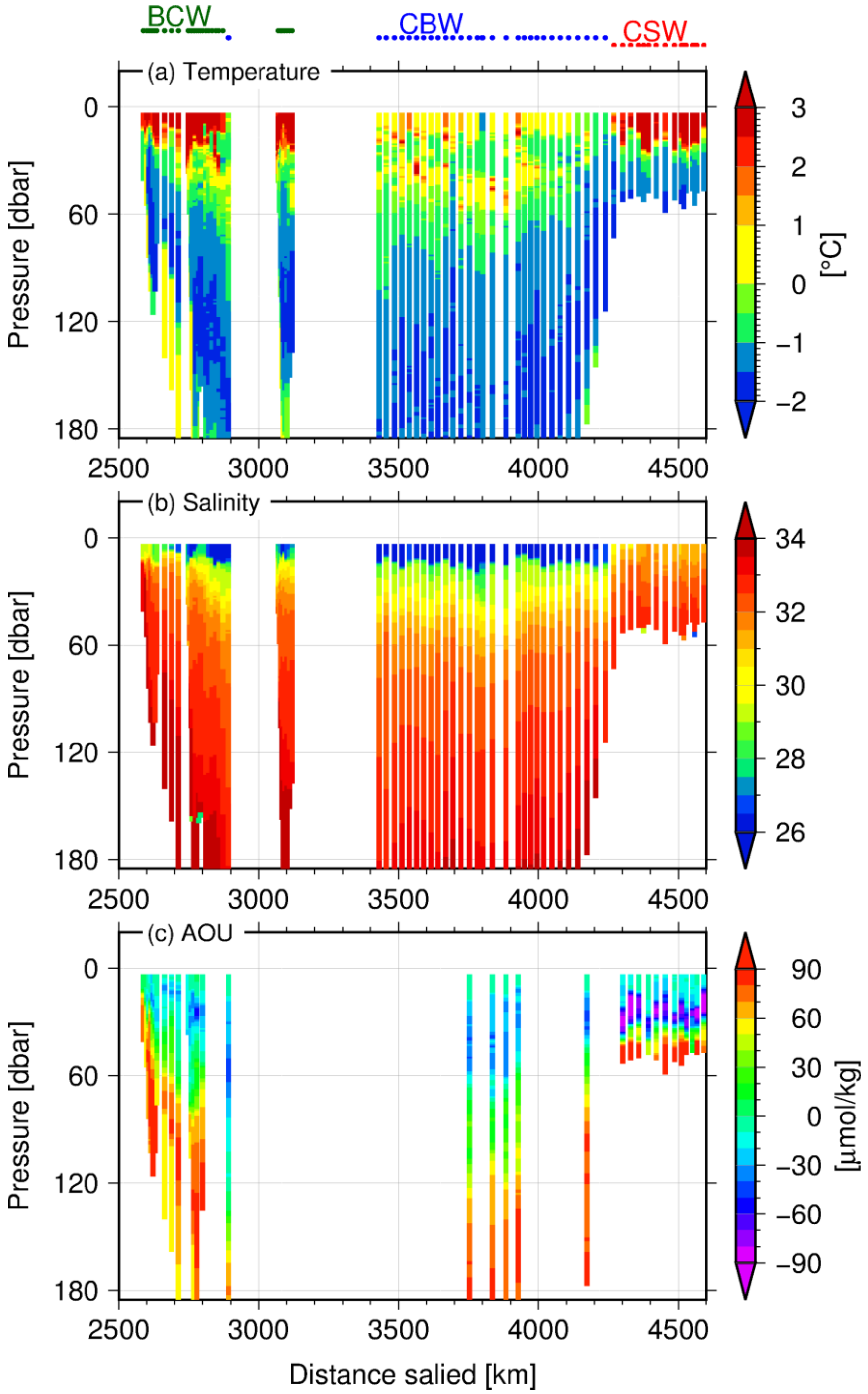

Figure 5 (revised) Column profiles of (a) temperature, (b) salinity, (c) apparent oxygen utilization (AOU), (d) pCO_2^{sea}, (e) f_{SIM}, and (f) f_{RRO} along the cruise track in the period 4–11 September 2013. Data were obtained by CTD and XCTD in (a) and (b), by oxygen sensor SBE 43 on CTD in (c), and by discrete bottle samples in (d), (e) and (f). Water types BCW (Barrow Coastal Water, CBW (Canada Basin Water), and CSW (Chukchi Sea Water) are indicated at the top of the figure.

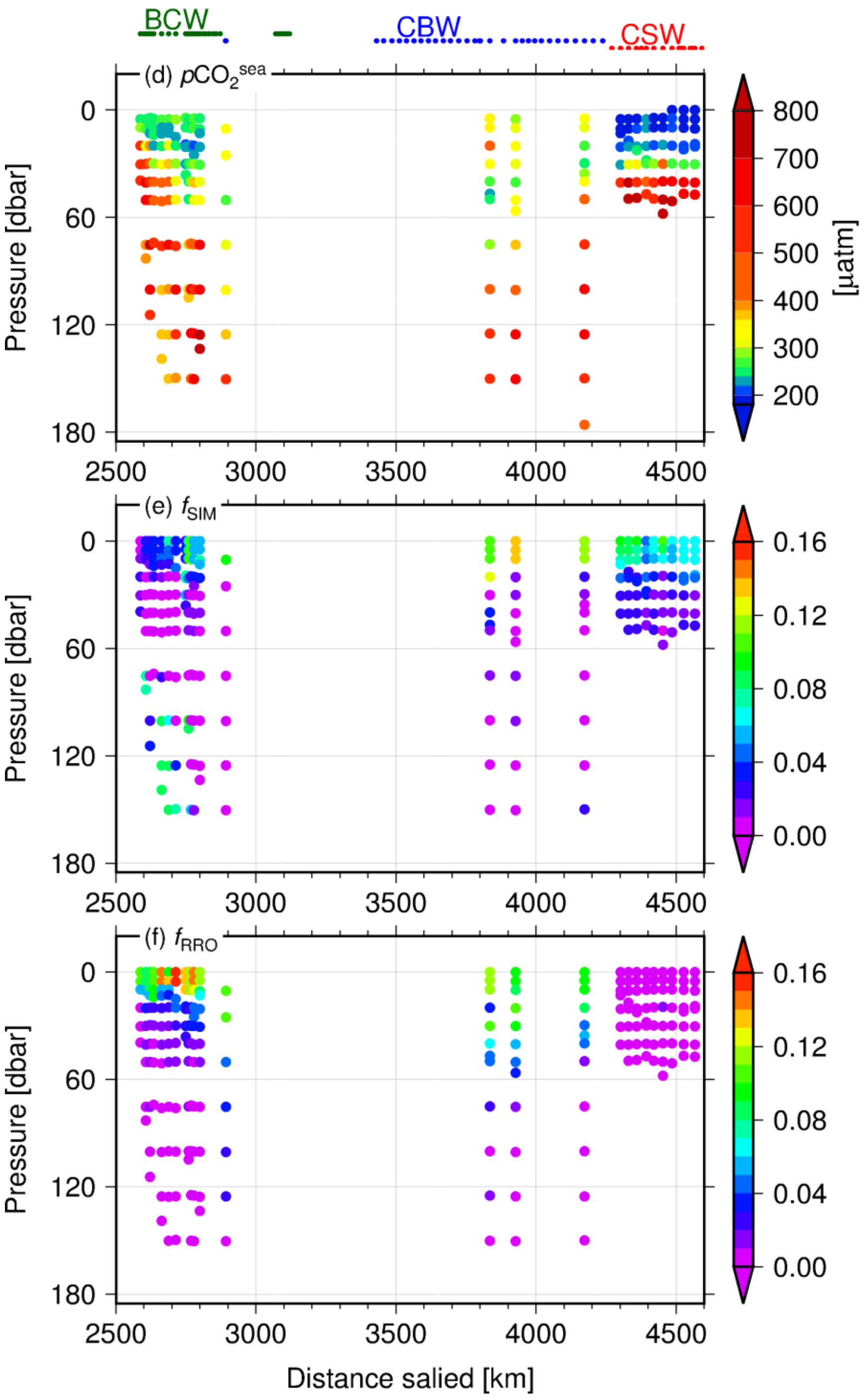

Figure 5 (revised; continued)

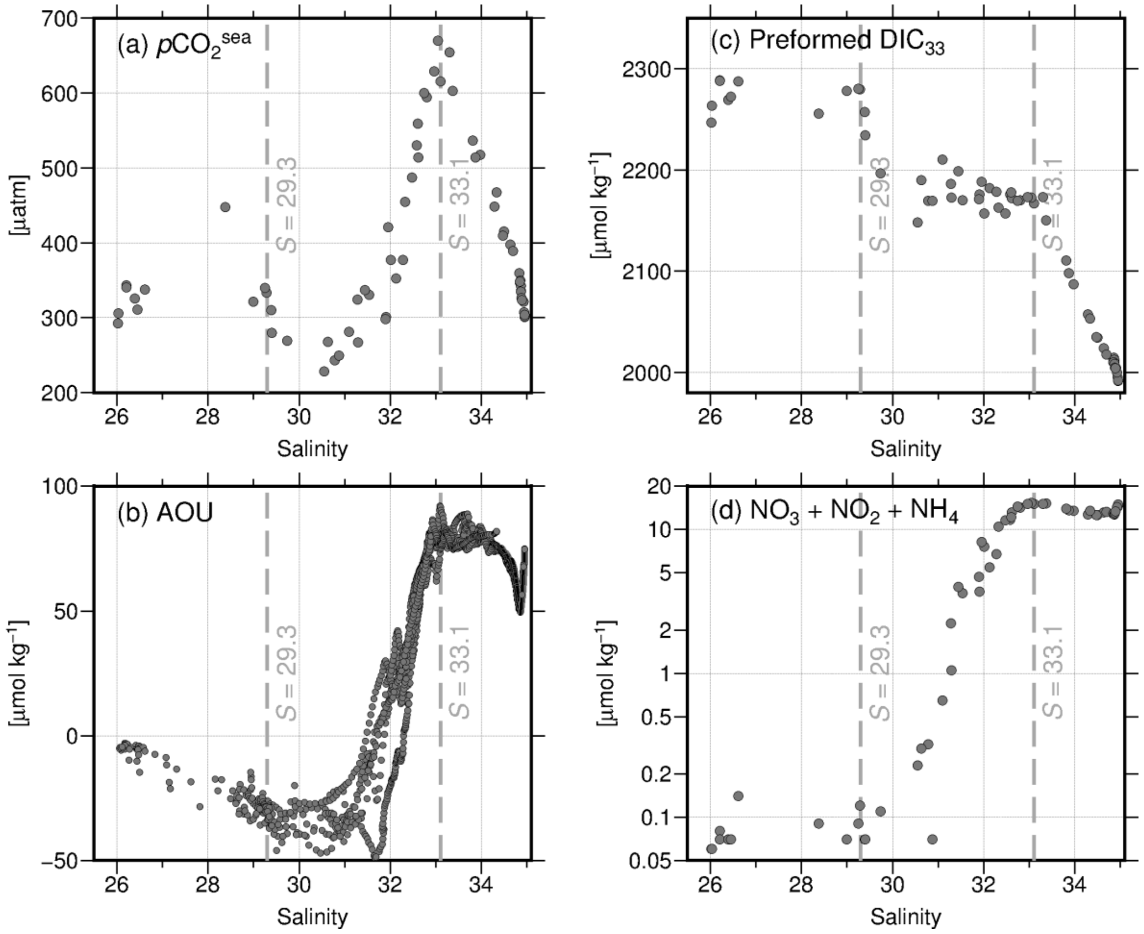

Figure 6 (revised) Property-property plots in the Canada Basin Water values for (a) salinity and $p\mathrm{CO}_2^{\mathrm{sea}}$ in discrete bottle samples, (b) salinity and apparent oxygen utilization (AOU) from CTD cast data, (c) salinity and preformed DIC (= {DIC - AOU} / S *32) in discrete bottle samples and (d) salinity and ($\mathrm{NO}_3 + \mathrm{NO}_2 + \mathrm{NH}_4$) in logarithmic scale in discrete bottle samples. Salinity of rWML (S = 29.3) and PWW (S = 33.1) were indicated as gray dotted lines.

First of all, we would like to thank reviewers for their valuable comments on our manuscript. We revised our manuscript carefully by taking these comments into account.

General comments:

The Arctic Ocean is a rapidly changing system that has a highly dynamic CO2 system both seasonally and with the changing physical conditions and climate change scenarios. The authors presented CO2 system data during an autumn of 2013 cruise which will enrich the available CO2 data in the Arctic Ocean and benefit the scientific community

(however the dataset is still available via the link). Their results largely support other recent observations that pCO2 is low in ocean margin but high (approaching to the atmospheric pCO2) in the Canada Basin. The explanations they provide are also consistent with other recent publications. Most interesting, the authors observed a subsurface minimal pCO2 structure in the Canada basin. They demonstrated this feature in fig. 5 and discussed the causes for low pCO2 water by analysis the water types, TA-S and pCO2-AOU relationships. Finally, they discussed the possible fate of this "hidden CO2 sink" and its influence in the future Arctic Ocean (they basically rejected this possibility, which I also agree). I agree with most of their views. Their finding is worthy to be published. However, the main conclusion in this paper is undermined because of not enough data, i.e. low pCO2 in the subsurface of Canada Basin. It is also not clear to me whether pCO2 minimum at 30-50m is due to in situ biological production as they have suggested or subduction of surface water from the highly productive shelf. I think more complete depth profiles from the Niskin bottle samples down to 150-200 m rather than 50m alone from a CTD pumping system will help to elucidate this issue.

Sections were expanded down to 180 m in order to cover PSW and PWW. Please see Figure 5 (revised) attached.

Another issue I have with this manuscript is writing. In general they have done a good job in writing except the text around Fig. 5. I don't think the authors put enough thinking into organizing the paper the best they can. One indication is they presented air-sea CO2 flux calculation method in the methods section but never presented air-sea CO2. Did they initially prepared a longer paper and then deleted the flux part?

As you mentioned, calculation of air-sea CO_2 flux is not the main theme of this paper. However, we have to mention how to calculate half-life of ΔpCO_2. We divided "Data and Methods" into two new sections, "Measurements and Data" and "Calculations". How to calculate the half-life and data used for calculation was described in "Calculations" section.

Another indication is in Fig. 5. While it is nice to see the pCO2 minimum with a high frequency depth profile, the depths of such profiles are limited to 50m. However the Pacific winter water and Pacific summer water are all deeper than 50m (if not in this region, they should say it). Thus the entire discussion is not clear. Most important, it is not clear to me whether pCO2 minimum at 30-50m is due to in situ biological production or subduction of surface water from the highly productive shelf. Again, I feel using the depth profile from the Niskin bottle based profiles will help to elucidate this issue. Such depth profiles will also present nutrient profiles to support the argument on nutrient availability (rather than just citing melting pond information). In summary I'd support the eventual publication of this paper but not at this stage. More data are needed to support their arguments.

In order to compare water properties, we calculated preformed nDIC_{32} using the following equation.

$$\text{preformed nDIC}_{32} = \frac{DIC - AOU * r_{C:O}}{S} \cdot 32$$

Stoichiometric respiration ratio of $\Delta CO_2/-\Delta O_2$ ($r_{C:O}$) was set to 117/170 (Anderson and Sarminento, 1994). Also concentrations of nutrients measured onboard were used for the analysis. Figure 6c and 6d were added and attached at the end of this reply. Preformed DIC_{32} and dissolved nitrate changed abruptly around S = 29.3. Above this layer, dissolved nitrate was almost depleted and preformed DIC_{32} was relatively high (~2200 μmol kg^{-1}). Significant nitrates remained and preformed DIC_{32} was low (~2100 μmol kg^{-1}) between S = 29.3 and S = 33.1. S = 29.3 corresponds to temperature minimum in the Canada Basin, i.e., rWML (Figure 4c). The layers rWML and above have been formed in the Canada Basin. PSW and PWW which were distributed between rWML and another temperature minimum around S = 33.1 were formed in the Chukchi Sea and subducted to the Canada Basin. Low $p\mathrm{CO}_2$ (< 300 matm) was mostly limited to the layer just below rWML. This layer corresponds to PSW. Therefore, low $p\mathrm{CO}_2$ under the halocline in the Canada Basin was attributable to the subduction of highly productive water from the Chukchi Sea rather than in situ production in the Canada Basin.

Specific comments

Page 1 Line 23 it is unnecessary to add "e.g." before the citation.

We removed "e.g.".

Page 2 Line 14 changing "reduces" to "limits"

We changed "reduces" to "limits".

Page3 The pCO2 data set presented in this paper is still not available to readers though the link: (http://www.godac.jamstec.go.jp/darwin/cruise/mirai/mr13-06_leg1/e).

We have submitted the data to data center of JAMSTEC. However, it has not been uploaded yet. We inquired the data center about it.

Equation 1 is totally unnecessary. Just cite Takahashi would be enough.

If the authors didn't do any calculation of CO2 flux in this paper, it is totally unnecessary to have the description of air-sea CO2 flux calculation (page 3, line 17- line 25).

Calculating regional air-sea CO_2 flux was not a goal of our paper. However, it is essential to mention about air-sea CO_2 flux since we calculated half-life of $\Delta p\mathrm{CO}_2$. Please see subsequent comment about the calculation of half-life.

Line 22, equation (4). I don't recall W92 has a non-zero term. Please check if you cited a more recent Wanninkhof paper and equation.

$k = 0.251 \cdot U_{10}^{2} \cdot (Sc/660)^{-0.5}$ was suggested in the most recent Wanninkhof's paper (Wanninkhof 2014). Also Scmidt number was updated to the latest value in Wannikhof (2014).

Line 24-25 The wind speed at 24 m height is measured by an anemometer and is extrapolated to 10m. Using an instantaneous wind speed is probably not the best choice for CO2 flux calculation with underway data. The average wind speed from satellite data may make more sense due to equilibrium time for CO2 is pretty long. For example, at 1 pm, if a vessel is at point A where pCO2 is 350 uatm and wind speed is 4 m/s. When the ship arrives at point B at 11 pm the same day where pCO2 is 350 uatm and wind speed increases to 7 m/s. It doesn't make any sense to believe that CO2 uptake flux is much greater at point B than A. If you will use satellite wind, then the fluxes in these two locations are likely the same (that is winds are same for A and B but only changes over a day). However, I must say since calculating flux is not the goal of this paper, this is not a serious problem. Then, of course, there would be no need for the authors to even present the flux calculation equation.

We used monthly averaged wind speed derived from climate reanalysis JRA-55 (Kobayashi et al., 2015). Wind speed in the Canada Basin in September 2013 ranged 4-5 m sec^{-1}. We divided "Data and Methods" into two new sections, "Measurements and Data" and "Calculations". Usage of JRA-55 was added to "Measurement and Data" section. Description about the correction from wind speed at 24 m to that at 10 m was removed.

Page 4 Line 17 What software or package was used for calculation of carbonate chemistry?

We used for macro package of CO2SYS program for Microsoft Excel. Usage and reference (Pierrot et al., 2006) were added.

Page5 Line 7 TARRO should be TARRO

"TARRO" was changed to "$\mathrm{TA}_{\mathrm{RRO}}$" according to your comment.

Line 22-24 The description of "(1) Barrow Coastal Water (BCW) was relatively warm and fresh

(SST > 2 , SSS < 30.5). (2) Canada Basin Water (CBW) was cold and fresh (SST < 2 C, SSS < 28). (3) Chukchi Sea Water (CSW) was saline (SSS > 28)" is a little confusing. BCW was fresh SSS<30.5 while CSW was saline (SSS>28). What is the reference for fresh and saline? As I see it (Fig. 3), most of BCW had SSS<28.5 except the very nearshore part while most CSW had SSS>30.5. Only minor clarification is needed here.

Difference in water properties between BCW and CBW was remarkable in temperature. On the other hand, that between CBW and CSW was remarkable in salinity. Therefore, we changed Line 21-25 to "We defined three subregions; (1) Barrow Coastal Water (BCW), (2) Canada Basin Water (CBW) and (3) Chukchi Sea Water (3). The boundary between BCW and CBW was 2°C isotherm at 72.5°N, 154.8°E. CBW and CSW was separated 28 psu isohaline at 73.3°N 168.3°E (Fig 3c)."

Page 6 Line 3 removing "the resulting" as low DIC/TA and low pCO2 are the same thing or same result of physical and biogeochemical processes (biological uptake here, but in the basin CO2 evasion from the atmosphere plus strong stratification and low PP in surface water). There is no magic low DIC/TA that leads to low pCO2.

Admittedly, "the resulting" was removed.

Line 9 regarding "half-life of CO2 gas exchange", while I can guess how did you estimate this, it is better to tell readers.

At first, initial condition of temperature, salinity, DIC, TA and mixed layer depth was set.

Initial $p\mathrm{CO}_2$ ($p\mathrm{CO}_2{}^0$) was calculated. Initial $\Delta p\mathrm{CO}_2$ ($\Delta p\mathrm{CO}_2{}^0$) was the difference between $p\mathrm{CO}_2{}^0$ and atmospheric $p\mathrm{CO}_2$ ($p\mathrm{CO}_2{}^{air}$).

$$pCO_2{}^0 = f(T,S,DIC,TA)$$

$$\Delta pCO_2^0 = pCO_2^0 - pCO_2^{air}$$

All parameter except DIC were fixed during the calculation, i.e. evaporation, precipitation and lateral/vertical advection were assumed unchanged. Flux of CO_2 (F_{CO2}) was calculated from wind speed and gas transfer coefficient. Time step was set to one day. Here, k and K_0 denote the solubility of CO_2 by Weiss (1974) and gas transfer coefficient by Wanninkhof (2014) respectively.

$$F_{CO2} = kK_0\Delta pCO_2$$

$$k = 0.251 \cdot U_{10}^2 \cdot (Sc/660)^{-0.5}$$

Increase in DIC in each time step was calculated from F_{CO2}.

$$\Delta \mathrm{DIC} = \frac{F_{CO2}}{MLD * \rho(T,\ S)}$$

$$DIC_{t+1} = DIC_t + \Delta DIC$$

Here, MLD and $\rho(T, S)$ mean mixed layer depth [m] and density of seawater in mixed layer [kg m^{-3}] respectively. After each time step, $p\mathrm{CO}_2{}^t$ and $\Delta p\mathrm{CO}_2{}^t$ were calculated from DIC at the time.

$$pCO_{2,t} = f(T, S, DIC_t, TA)$$

$$\Delta pCO_2^t = pCO_2^t - pCO_2^{air}$$

Half-life means the time required to reduce$\Delta p\mathrm{CO}_2^{t}$ to half of $\Delta p\mathrm{CO}_2^{0}$. Description of these processes for calculation of half-life was added to “Calculation” section.

Line 17 Font is different from other context Nutrient in melting pond cannot be a sufficient evidence for limitation of nitrate in surface water. Report directly the nutrient data in water would be better.

We used nutrients data measured on the ship to prepare Figure 6d. In this figure, nutrients depletion (nitrates < 0.2 μmol kg^{-1}) above S = 29.3 (i.e., Canada Basin origin water) and presence of nutrients (about 1 μmol kg^{-1} at S = 31) in Pacific origin water are presented.

Line 24 change “pCO2sea” to “pCO2sea ”

We changed “$p\mathrm{CO}_2$sea” to ”$p\mathrm{CO}_2^{\mathrm{sea}}$”.

Line 29-30 “Reduction in CO2 absorption capacity by riverine discharge was not as large as that by sea-ice melt.” This conclusion is not solid. Need more explicit verification.

Difference in $p\mathrm{CO}_2$ between BCW and CBW was attributable to DIC rather than fraction of fresh water. Please see newly drawn Figure AC1. Relation between F_{RRO} and nDIC_{32} was almost linear in BCW and CSW. However, CBW indicated positive anomaly of nDIC_{32} from linear relation. Additional DIC was imposed on only CBW by possibly air-sea CO_2 flux. As a result, “Reduction in CO_2 absorption capacity by riverine discharge was not as large as that by sea-ice melt.” was partly incorrect. It was replaced by “At the time of the observation, BCW still could absorb more atmospheric CO_2 than offshore CBW”.

Page 7 Line 4 changing “with depth” to “as depth increases”

We changed “with depth” to “as depth increases”.

Line 17-18 “In CSW, the halocline, although not as clear as in the other two subregions, was at almost the same depth.” But thermocline is very obvious in CSW (Figure 5a).

In CSW, the halocline, although not as clear as in the other two subregions, was at almost the same depth.” was changed to “Unlike the other two subregions, thermocline was more prominent than halocline in CSW.”

Line 21 Should “In contrast” be “Likewise”? not clear what is the undertone by this.

“In contrast” was changed to “Likewise”.

Page 7 line 19, what is “column variation”? must be water column? Same in lines 26, 29 and 31, all change to “water” column profiles.
All “column profile” were changed to “water column profile”.

p.7 Line 26- Page 8 Line 12 The biggest problem here is pCO2 data in CBW is too limited. (only three water column data shown in Figure 5e). Considering the mixing layer structure is complicated in this subregion, it is difficult to see the real pattern. With only 3 station, how to distinguish the real reasons for low pCO2 in subsurface CBW, either due to the local net primary production in CBW or just the water with low pCO2 subducted and advected into the Canada Basin? If the authors could plot the entire water column data (deeper than 50 m in Figure 5), that would provide more information and be helpful to interpret their finding. Also, the Discussion of various waters does not related to Fig. 5 very well, thus causing confusion in reading as the deepest depth is only 50m while the winter water (rWML) is about 120m and summer water (PSW) is even deeper. I am somewhat confused in reading lines 5-13 in p. 8. Since this part is the new point that the authors want to present. It absolutely should be explained very clearly.
Temperature minimum layer around S = 29.3 in Figure 5 was rWML. PSW was relatively warm water just below rWML to temperature maximum around S = 31. As shown in Figure 6a, $p\mathrm{CO}_2^{\mathrm{sea}}$ showed small variability ranging 300-350 μatm in the layers shallower than S = 29.3. The lowest $p\mathrm{CO}_2^{\mathrm{sea}}$ was seen in the water of 29 < S < 31. This layer was PSW which was formed in the Chukchi Sea and advected to the Canada Basin. Subsurface minimum in $p\mathrm{CO}_2^{\mathrm{sea}}$ in the Canada Basin was formed due to biological production in subducted PSW rather than in Canada Basin origin water. This was supported by low preformed nDIC_{32} (Figure 6c) and existence of nutrients (Figure 6d) in Pacific origin water between S = 29.3 and S = 33.1.

p.8, line 30, replace “think” with “believe” or “suggest”.
We changed “think” to “suggest”.

Table 1 It is not clear whether the average of all the samples were within mixing layer or including the entire water columns. It is probably better to separate the data into mixing layer and below mixing layer for discussion. And please add standard deviation.
All data in Table 1 was for surface water pumped from ship’s bottom. This information was added to the caption of Table 1. Standard deviation was added to Table 1 (please see below).

Reference

Anderson, L. A. and J. L. Sarmiento, (1994), Redfield ratios of remineralization determined by nutrient data analysis, Global Biogeochemical Cycles, 8, 65-80.

Kobayashi, S., Y. Ota, Y. Harada, A. Ebita, M. Moriya, H. Onoda, K. Onogi, H. Kamahori, C. Kobayashi, H. Endo, K. Miyaoka, and K. Takahashi, (2015), The JRA-55 Reanalysis: General specifications and basic characteristics. J. Meteor. Soc. Japan, 93, 5-48, doi:10.2151/jmsj.2015-001.

Pierrot, D. E. Lewis, and D. W. R. Wallace. (2006), MS Excel Program Developed for CO2 System Calculations. ORNL/CDIAC-105a. Carbon Dioxide Information Analysis Center, Oak Ridge National Laboratory, U.S. Department of Energy, Oak Ridge, Tennessee. doi: 10.3334/CDIAC/otg.CO2SYS_XLS_CDIAC105a

Wanninkhof, R., (2014), Relationship between wind speed and gas exchange over the ocean revisited, Limnology and Oceanography: Methods, 12, 351-362, doi: 10.4319/lom.2014.12.351.

Table 1 (revised)

Summary of three water types (BCW; Barrow Coastal Water, CBW; Canada Basin Water and CSW; Chukchi SeaWater) at the surface. All sample waters were pumped up underway from an intake at ship's bottom. Values are averages for samples collected from 4 to 11 September 2013. N denotes the number of samples. nDIC$_{32}$ and nTA$_{32}$ are DIC and TA normalized to S =32 respectively (nDIC$_{32}$ = DIC / S · 32; nTA$_{32}$ = TA / S · 32). Standard deviation (SD) was listed below each value.

Water Type	N	T [°C]	S	DIC [µmol kg^{-1}]	nDIC$_{32}$ [µmol kg^{-1}]	pCO$_2$ [µatm]	TA [µmol kg^{-1}]	nTA$_{32}$ [µmol kg^{-1}]	DIC/TA	f_{RRO}	f_{SIM}
BCW	109	2.88	27.01	1827	2166	274	1948	2309	0.938	0.11	0.08
(SD)		0.30	1.37	72	34	13	85	25	0.006	0.02	0.04
CBW	118	0.66	26.19	1803	2203	332	1882	2299	0.958	0.10	0.12
(SD)		0.58	0.24	19	16	19	16	9	0.004	0.01	0.01
CSW	54	3.03	31.06	1923	1982	198	2131	2196	0.903	-0.01	0.08
(SD)		0.23	0.19	13	6	19	12	3	0.002	0.00	0.01

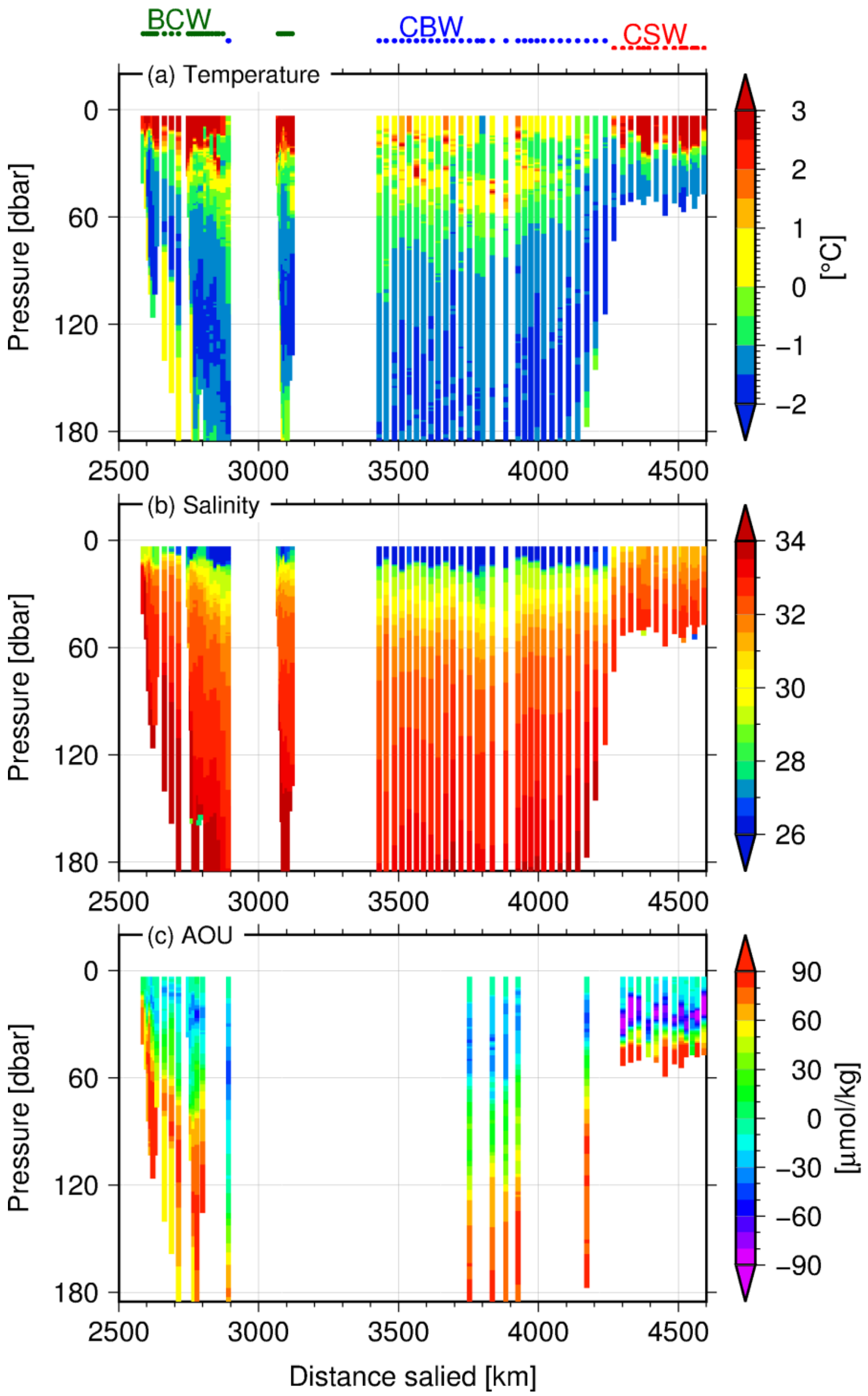

Figure 5 (revised) Column profiles of (a) temperature, (b) salinity, (c) apparent oxygen utilization (AOU), (d) pCO_2^{sea}, (e) f_{SIM}, and (f) f_{RRO} along the cruise track in the period 4–11 September 2013. Data were obtained by CTD and XCTD in (a) and (b), by oxygen sensor SBE 43 on CTD in (c), and by discrete bottle samples in (d), (e) and (f). Water types BCW (Barrow Coastal Water, CBW (Canada Basin Water), and CSW (Chukchi Sea Water) are indicated at the top of the figure.

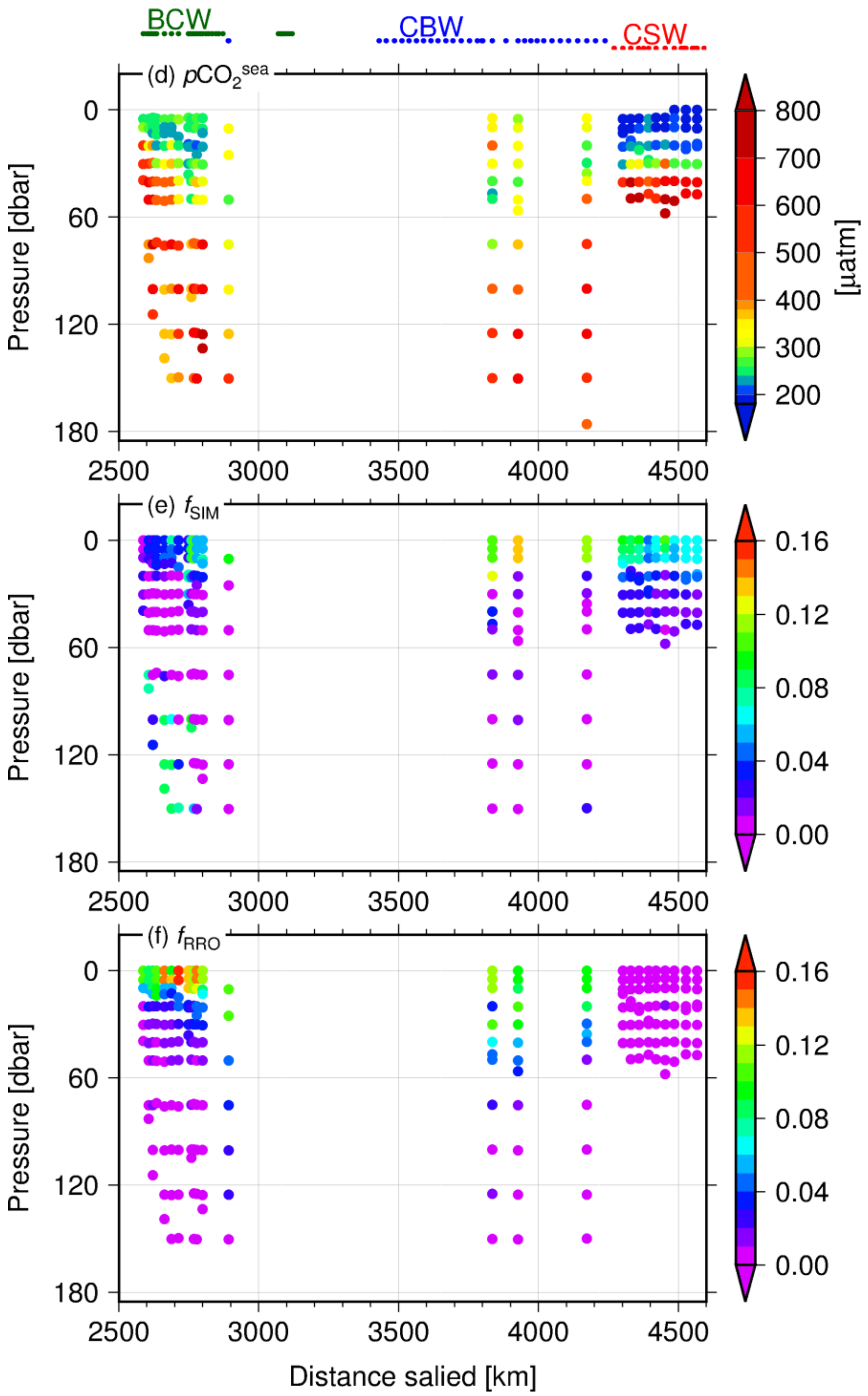

Figure 5 (revised; continued)

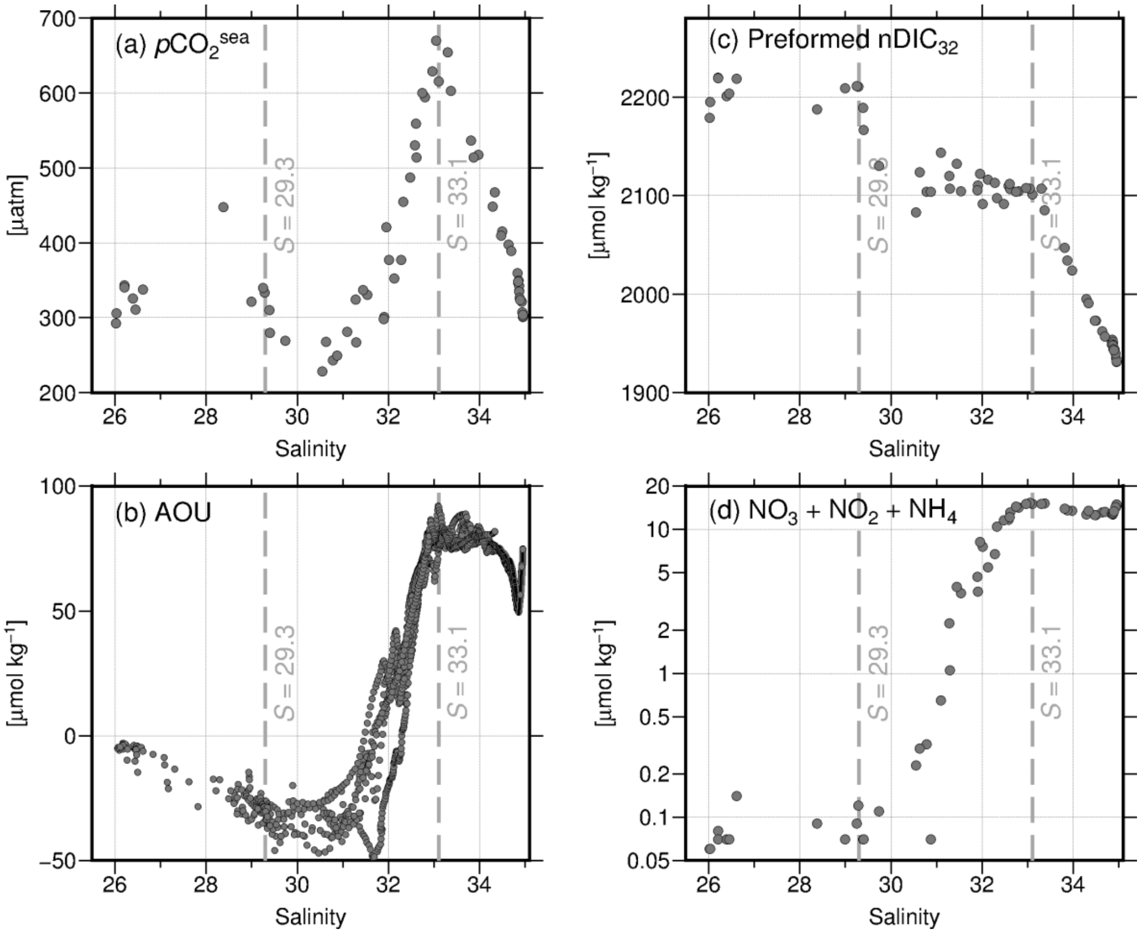

Figure 6 (revised) Canada Basin Water values for (a) salinity and pCO_2^{sea} in discrete bottle samples, (b) salinity and apparent oxygen utilization (AOU) from CTD cast data, (c) salinity and preformed $nDIC_{32}$ (= {DIC – AOU} / $S \cdot 32$) in discrete bottle samples and (d) salinity and ($NO_3 + NO_2 + NH_4$) in logarithmic scale in discrete bottle samples. Salinity of rWML (S = 29.3) and PWW (S = 33.1) were indicated as gray dotted lines.

Low $p\mathrm{CO}_2$ under sea-ice melt in the Canada Basin of the western Arctic Ocean

Naohiro Kosugi[1], Daisuke Sasano[2], Masao Ishii[1], Shigeto Nishino[3], Hiroshi Uchida[3], Hisayuki Yoshikawa-Inoue[4]

[1]Meteorological Research Institute, Tsukuba, 305-0052, Japan
[2]Japan Meteorological Agency, Tokyo, 100-8122, Japan
[3]Japan Agency for Marine-Earth Science and Technology, Yokosuka, 237-0061, Japan
[4]Hokkaido University, Sapporo, 060-0810, Japan

Correspondence to: Naohiro Kosugi (nkosugi@mri-jma.go.jp)

Abstract. In September 2013, we observed an expanse of surface water with low CO_2 partial pressure ($p\mathrm{CO}_2^{\mathrm{sea}}$) (< 200 μatm) in the Chukchi Sea of the western Arctic Ocean. The large undersaturation of CO_2 in this region was the result of massive primary production after the sea-ice retreat in June and July. In the surface of the Canada Basin, salinity was low (< 27) and $p\mathrm{CO}_2^{\mathrm{sea}}$ was closer to the air–sea CO_2 equilibrium (~360 μatm). From the relationships between salinity and total alkalinity, we confirmed that the low salinity in the Canada Basin was due to the larger fraction of meltwater input (~0.16) rather than the riverine discharge (~0.1). We attribute the relatively high $p\mathrm{CO}_2^{\mathrm{sea}}$ in the Canada Basin to the shallow mixed layer and limited net primary production. Such an increase in $p\mathrm{CO}_2^{\mathrm{sea}}$ was not so clear in the coastal region near Point Barrow, where the fraction of riverine discharge was larger than that of ~~sea-~~sea-ice melt. We also identified low $p\mathrm{CO}_2^{\mathrm{sea}}$ (< 250 μatm) under the halocline of the Canada Basin. ~~Oxygen supersaturation in t~~This subsurface low $p\mathrm{CO}_2^{\mathrm{sea}}$ is attributed to the advection of Pacific-origin water, in which DIC is relatively low, through the Chukchi Sea where net primary production is high. ~~layer corroborates that the decrease in $p\mathrm{CO}_2^{\mathrm{sea}}$ was due to net primary production.~~ If these low $p\mathrm{CO}_2^{\mathrm{sea}}$ layers surface by wind mixing, they will act as additional CO_2 sinks; however, this is unlikely because intensification of stratification by sea-ice melt inhibits mixing across the halocline.

1 Introduction

The extent of sea ice and its thickness in the Arctic Ocean have been declining in recent decades (~~e.g.,~~ Comiso, 2012; Stroeve et al., 2012a, 2012b); these declines are widely considered a consequence of climate change resulting from the emissions of anthropogenic greenhouse gases. The average monthly extent of sea ice in September in the Arctic Ocean decreased by about 12.4% per decade from 1979 to 2010 (Stroeve et al., 2012b). In September 2012, the area of sea ice in the Arctic Ocean was less than 4×10^6 km^2, about 50% of the average in the 1980s (Parkinson and Comiso, 2013). Because of this decline in the extent of sea ice, the air–sea CO_2 flux in the Arctic Ocean is also thought to be dramatically changing. Currently, the Arctic CO_2 sink has been estimated as 66–199 Tg C yr^{-1}, with a large uncertainty (Bates and Mathis, 2009).

This value is equivalent to 3–8% of the net CO_2 sink of the global ocean (2.6 ± 0.5 Pg C yr^{-1} in the period 2006–2015; Le Quéré et al., 2016). A recent modeling study suggests that the CO_2 sink in the Arctic Ocean is increasing (Manizza et al., 2013).

The reasons for an increasing CO_2 sink in the Arctic Ocean include the increase in the area and duration of ice-free conditions and the enhanced net primary production they induce. However, the effect of increasing meltwater input that accompanies the sea ice decline should also be taken into consideration (e.g., Yamamoto-Kawai et al., 2009; Rabe et al., 2014). The large input of ice melt enhances stratification in the upper layer and forms a thin surface mixed layer with a distinct halocline below. Although dilution of the surface water with meltwater lowers the partial pressure of CO_2 ($p\mathrm{CO_2}^{\mathrm{sea}}$), shoaling of the surface mixed layer would accelerate equilibration of the surface water with the overlying air. The input of meltwater is also likely to influence carbonate chemistry by altering the ratio of dissolved inorganic carbon (DIC) to total alkalinity (TA), although it is still unclear whether the addition of meltwater increases or decreases the DIC/TA ratio (Rysgaard et al., 2007; Bates et al., 2014). Cai et al. (2010) reported unprecedented high $p\mathrm{CO_2}^{\mathrm{sea}}$ (~370 μatm) in the Canada Basin in summer. They ascribed this high $p\mathrm{CO_2}^{\mathrm{sea}}$ to low net primary production and rapid equilibration with atmospheric CO_2 in the shallow mixed layer derived from meltwater input. The low nutrient content in meltwater ~~reduces~~limits the biological drawdown of $p\mathrm{CO_2}^{\mathrm{sea}}$. Else et al. (2013) found that surface warming also contributed significantly to $p\mathrm{CO_2}^{\mathrm{sea}}$ increase in a shallow mixed layer in the Canada Basin. Both studies concluded that an increase in meltwater lowers CO_2 absorbing capacity in the Canada Basin.

A notable feature of the Canada Basin in summer is a complex water column structure. Because of the strong salinity gradient, there are several maxima and minima of temperature within 150 m of the surface. This water column structure does not always remain stable in the rapidly changing Arctic Ocean. Although Cai et al. (2010) and Else et al. (2013) reported relatively high surface $p\mathrm{CO_2}^{\mathrm{sea}}$ in the Canada Basin, they did not fully explain the CO_2 chemistry below the surface mixed layer there. We studied the water column CO_2 variation in the western Arctic Ocean and the processes that cause it.

In late summer 2013, we made shipboard observations in the Chukchi Sea and in the Canada Basin of the western Arctic Ocean. While underway or at hydrographic stations, or both, we measured temperature, salinity, dissolved oxygen, and the carbonate system variables $p\mathrm{CO_2}^{\mathrm{sea}}$, DIC, and TA. From the salinity–TA relationship, we also mapped the mixing ratio of sea-ice meltwater, riverine outflow, and a water of Pacific origin that entered into the western Arctic Ocean through the Bering Strait. The results demonstrate the importance of large net primary production in reducing the $p\mathrm{CO_2}^{\mathrm{sea}}$ and increasing air-to-sea CO_2 flux in the Chukchi Sea. Although this low $p\mathrm{CO_2}^{\mathrm{sea}}$ water is advected into the Canada Basin, air-to-sea CO_2 flux there is blocked by a stratified shallow surface layer that is formed by a large ice-melt input.

2. ~~Data and Methods~~Measurements and Data

Oceanographic measurements in the Chukchi Sea and the Canada Basin were made during cruise MR13-06 of the R/V *Mirai* conducted by the Japan Agency for Marine-Earth Science and Technology from 28 August to 6 October 2013 (Nishino et al., 2015). The port of departure and arrival was Dutch Harbor, Alaska, USA. ~~The~~ Most of data used in this paper are available from the JAMSTEC Data Site for Research Cruises (http://www.godac.jamstec.go.jp/darwin/cruise/mirai/mr13-06_leg1/e). The rest of the data will be opened as soon as they are ready.

We made underway measurements of $p\mathrm{CO}_2^{\mathrm{sea}}$ and DIC together with temperature (T) and salinity (S) in seawater pumped continuously from an intake located 4.5 m below surface. For the measurement of $p\mathrm{CO}_2^{\mathrm{sea}}$, the pumped water was continuously introduced into a shower-type equilibrator with 1.4 dm^3 headspace at a rate of 4 $\mathrm{dm}^3\ \mathrm{min}^{-1}$. A wavelength-scanned cavity ring-down spectrometer (Picarro G2301, Picarro Inc., USA) was used to measure the concentrations of CO_2 in the headspace of the equilibrator and in the atmosphere ~~(~~sampled from the foremast~~)~~. The instrument was stable and calibrated once a day against a set of three working standard gases of CO_2 in air (Japan Fine Products, 206.34 to 489.28 ppmv) that had been standardized on the WMO X2007 scale (Zhao and Tans, 2006). Response of the instrument to the CO_2 concentration was practically linear. The residual of each standard gas from liner regression was less than 0.03 ppmv. According to the manufacturer's report, precision of CO_2 measurement above 500 ppmv is 0.1%. ~~Surface $p\mathrm{CO}_2^{\mathrm{sea}}$ was calculated from the mole fraction of CO_2 in the air by taking the water vapor pressure and atmospheric pressure into account. The temperature and salinity of the pumped water at the intake were continuously measured with sensors SBE 38 and SBE 45, respectively (Sea-Bird Electronics, USA). PT100 thermometer was equipped with the equilibrator. An increase in temperature between in situ seawater (T_{in}) and the equilibrator (T_{eq}) was typically about 0.2 °C. Equation (1) proposed by Takahashi et al. (2009) was applied to convert $p\mathrm{CO}_2(T_{\mathrm{eq}})$ to $p\mathrm{CO}_2(T_{\mathrm{in}})$,~~

~~$p\mathrm{CO}_{2(\mathrm{Tin})} = p\mathrm{CO}_{2(\mathrm{Teq})} \times \exp\,[0.0433(T_{\mathrm{in}} - T_{\mathrm{eq}}) - 4.35 \times 10^{-5}\{(T_{\mathrm{in}})^2 - (T_{\mathrm{eq}})^2\}]$ (1)~~

~~Uncertainty in the value of $p\mathrm{CO}_2^{\mathrm{sea}}$ measured using the same type of equilibrator has been estimated to be ±3 μatm (Midorikawa et al., 2006).~~

~~Air–sea CO_2 flux (F_{CO2}) was calculated using the following equation:~~

~~$\Delta p\mathrm{CO}_2 = p\mathrm{CO}_2^{\mathrm{sea}} - p\mathrm{CO}_2^{\mathrm{air}}$ (2)~~

~~$F_{\mathrm{CO2}} = k\alpha\Delta p\mathrm{CO}_2$ (3)~~

~~where α denotes the solubility of CO_2 in seawater (Weiss 1974). We used a gas-transfer piston velocity k given by Wanninkhof (1992):~~

~~$k = \{2.5(0.5246 + 1.6256 \times 10^{-2}t + 4.9946 \times 10^{-4}t^2) + 0.3 \times U_{10}^{\ 2}\} \times (Sc \,/\, 660)^{-0.5}$ (4)~~

~~t, U_{10}, and Sc denote temperature of seawater (in degrees Celsius), wind speed at 10 m above sea level, and the Schmidt number, respectively. An anemometer was located on the foremast at 24 m above sea level. U_{10} was determined by multiplying the wind speed measured by the anemometer by $(10/24)^{0.11}$ (Hsu et al., 1994).~~

For the underway measurement of DIC, a portion of pumped water was automatically taken every 15 minutes and filled ~~automatically~~ into glass bottles (SCHOTT DURAN®; 300 cm^3) ~~every 15 minutes.~~ that have been capped with a screw type lid. Filling, transport and discharge of the samples were all done through high-density PFA-tubes mounted through the lid. DIC was measured after the temperature of the sample seawater was adjusted to 20.0 °C in a thermostated water bath for 1 hour, using a $\mathrm{CO_2}$ extraction/coulometric titration system (Nippon ANS, Inc., Japan). This system was comprised of seawater dispensing unit, a $\mathrm{CO_2}$ extraction unit, and a coulometer (Model 3000, Nippon ANS, Inc., Japan). The dispensing unit dispenses the seawater from sample bottle to a water-jacketed glass pipette of nominal 15 cm^3 volume. The temperature of seawater sample in the pipette was kept at 20.0 °C by a water jacket. The sample seawater was then transferred into a glass stripping chamber and stripped of DIC by adding 2 cm^3 of phosphoric acid (10% v/v). The emerged $\mathrm{CO_2}$ was extracted into the stream of nitrogen gas (130 cm^3 min^{-1}) and transferred to the coulometer. The system was standardized with Certified Reference Material (CRM; Batch #113) supplied by A. G. Dickson (Scripps Institution of Oceanography); underway measurement of DIC was interrupted for several hours once a day for calibration. The precision of measurement determined by repeatability of CRMs was ±2.2 μmol kg^{-1}. The values of TA in the surface were calculated from measured $p\mathrm{CO}_2^{\mathrm{sea}}$, DIC, temperature and salinity using dissociation constants of carbonic acid given by Lueker et al. (2000) and macro package of CO2SYS program for Microsoft Excel (Pierrot et al., 2006). Uncertainty in surface TA was estimated as ±3 μmol kg^{-1} by taking the uncertainties of DIC and $p\mathrm{CO}_2^{\mathrm{sea}}$ into account.

At hydrographic stations, seawater column profiles of temperature, salinity, and dissolved oxygen were obtained with a CTD (SBE 9 plus, Sea-Bird Scientific, USA) rosette sampler equipped with sensors for dissolved oxygen (SBE 43, Sea-Bird Scientific, USA) and Niskin bottles (12 dm^3). In addition to the CTD casts, some expendable CTDs (XCTD) were used to obtain water column profiles of temperature and salinity. Discrete water samples were taken into Niskin bottles ~~at depths~~ at ~~along with CTD measurements.~~ depths of 0, 5, 10, 20, 30, 40, 50, 75, 100, 125, 150 and 200 m along with CTD measurements. Samples were also collected at chlorophyll maximum layers that ranged from 12 m to 92 m. Measurements of dissolved oxygen were made by the Winkler titration method following Dickson (1994) and used to correct for the bias of the data from the oxygen sensor SBE 43. Apparent oxygen utilization (AOU), *i.e.*, the difference between the measured concentration of dissolved oxygen and its saturation concentration under the same ~~physical~~ potential temperature and salinity conditions, was calculated using the oxygen solubility constant given by Garcia and Gordon (1992). Water samples for chlorophyll a were vacuum-filtered (< 0.02 MPa) through a 25-mm-diameter Whatman grade GF/F filter, and fluorescence was measured for each sample with a fluorometer (10-AU-005, Turner Designs, USA). The fluorometer was calibrated against pure chlorophyll-*a* (Sigma-Aldrich, USA). The concentration of nutrients (nitrate, nitrite, silicate, phosphate and ammonia) was determined using a continuous flow analyzer (QuAAtro 2-HR, BLTEC, Japan) according to the GO-SHIP Repeat Hydrography Manual (Hydes et al., 2010). Reference materials for nutrients of seawater (Aoyama and Hydes, 2010) were used.

Subsamples for DIC and TA measurements in the discrete water samples were drawn into borosilicate glass bottles (300 cm^3 for DIC and 125 cm^3 for TA) using the protocol of Dickson et al. (2007). Measurements of DIC at depths were also made with the extraction/coulometric system (Nippon Ans., Japan). Saturated solution of $HgCl_2$ (0.1 cm^3) was added to each of the samples to inhibit any biological activity. Measurements of TA were made with a spectrophotometric system (Nippon Ans., Japan) based on a single-point pH determination using bromocresol green as an indicator dye (Yao and Byrne, 1998). Seawater sampled in the glass bottles was transferred to an optical cell via dispensing unit. The length and volume of the cell were 8 cm and 13 cm^3, respectively. Temperature of the cell was kept at 25.0 °C. Sample was mixed for 8.5 minutes after the injecting the indicator dye solution and hydrochlonic acid (0.05M). TA was calculated from absorbance ratio at 444 and 616 nm (A_{616}/A_{444}). Replicate measurements yielded an average and standard deviation of differences of 1.0 ± 1.1 μmol kg^{-1} for DIC and 0.9 ± 0.8 μmol kg^{-1} for TA. Values of $p\mathrm{CO_2}^{\mathrm{sea}}$ in discrete water samples were calculated from DIC, TA, temperature, and salinity using dissociation constants of carbonic acid given by Lueker et al. (2000).

Satellite-derived net primary production (NPP) was used to evaluate biological production in a broad area. NPP is estimated from empirical equations using chlorophyll concentration, sea surface temperature, photosynthetically active radiation and length of the daytime as variables in Vertical Generalized Production Model (Bahrenfeld and Falkowski, 1997). The data of NPP was downloaded from website of Oregon State University (http://www.science.oregonstate.edu/ocean.productivity/standard.product.php).

Monthly averaged wind speed data from the Japanese 55 year reanalysis (JRA-55) product was used to calculate air-sea CO_2 flux. JRA-55 has a spatial resolution of 1.25° longitude by 1.25° latitude (Kobayashi et al., 2015). We applied data of reanalysis rather than those of an anemometer mounted on the ship considering the representativeness of data.

3. Calculations

3.1 CO_2 flux and half-life of $\Delta p\mathrm{CO_2}$

Surface $p\mathrm{CO_2}^{\mathrm{sea}}$ was calculated from the mole fraction of CO_2 in the air by taking the water vapor pressure and atmospheric pressure into account. The temperature and salinity of the pumped water at the intake were continuously measured with sensors SBE 38 and SBE 45, respectively (Sea-Bird Electronics, USA). PT100 thermometer was equipped with the equilibrator. An increase in temperature between in situ seawater (T_{in}) and the equilibrator (T_{eq}) was typically about 0.2 °C. Equation (1) in~~proposed by~~ Takahashi et al. (2009) was applied to convert $p\mathrm{CO_2}(T_{\mathrm{eq}})$ to $p\mathrm{CO_2}(T_{\mathrm{in}})$. ~~:~~

~~$p\mathrm{CO}_{2(\mathrm{Tin})} = p\mathrm{CO}_{2(\mathrm{Teq})} \times \exp [0.0433(T_{\mathrm{in}} - T_{\mathrm{eq}}) - 4.35 \times 10^{-5} \{(T_{\mathrm{in}})^2 - (T_{\mathrm{eq}})^2 \}]$ (1)~~

Uncertainty in the value of $p\mathrm{CO_2}^{\mathrm{sea}}$ measured using the same type of equilibrator has been estimated to be ±3 μatm (Midorikawa et al., 2006).

Air–sea CO_2 flux (F_{CO2}) was calculated using the following equation:

$$\Delta p\mathrm{CO_2} = p\mathrm{CO_2}^{\mathrm{sea}} - p\mathrm{CO_2}^{\mathrm{air}} \qquad (~~2~~1)$$

$$F_{\mathrm{CO2}} = k\alpha\Delta p\mathrm{CO_2} \qquad (~~3~~2)$$

where α denotes the solubility of CO_2 in seawater (Weiss 1974). We used a gas-transfer piston velocity k given by Wanninkhof (~~1992~~2014):

$$k = 0.251\cancel{\{2.5(0.5246 + 1.6256 \times 10^{-2}t + 4.9946 \times 10^{-4}t^{2}) + 0.3 \times}\ U_{10}^{2}\cancel{\}} \times (Sc/660)^{-0.5}$$ (~~(4~~3)

~~t,~~ U_{10}, and Sc denote ~~temperature of seawater (in degrees Celsius),~~ wind speed at 10 m above sea level, and the Schmidt number (Wanninkhof, 2014), respectively.

Half-life of CO_2 gas exchange ($\tau_{1/2}$) was calculated for quantitative discussion about temporal variation in $\Delta p\mathrm{CO}_2$. At first, initial condition of temperature, salinity, DIC and TA were set. Initial $p\mathrm{CO}_2$ ($p\mathrm{CO}_2^0$) was calculated from these values using dissociation constants of carbonic acid given by Lueker et al. (2000).

$$p\mathrm{CO}_2^0 = f(T, S, DIC, TA) \qquad (4)$$

All parameters but DIC were fixed during the calculation, i.e., temperature, salinity and TA were assumed unchanged. F_{CO2} in each time step was calculated using equation (2), (3) and (4). Increase in DIC was calculated from F_{CO2}. Time step was set to one day.

$$\Delta\mathrm{DIC} = \frac{F_{\mathrm{CO2}}}{MLD * \rho(T,S)} \qquad (5)$$

$$DIC_{t+1} = DIC_t + \Delta DIC \qquad (6)$$

Here, MLD and (T, S) mean fixed mixed layer depth [m] and density of seawater in surface mixed layer [kg m^{-3}] respectively. After each time step, $\Delta p\mathrm{CO}_2^t$ and $p\mathrm{CO}_2^t$ were calculated from DIC. Time required to reduce $\Delta p\mathrm{CO}_2^t$ to half of $\Delta p\mathrm{CO}_2^0$ was defined as $\tau_{1/2}$.

3.2 Determination of freshwater fraction

~~**An anemometer was located on the foremast at 24 m above sea level. U_{10} was determined by multiplying the wind speed measured by the anemometer by $(10/24)^{0.11}$ (Hsu et al., 1994).**~~

In the western Arctic Ocean, the water at the temperature minimum layer (~150 dbar) is known to originate in the North Pacific and be advected into the Arctic through the Bering Strait (POW: Pacific Origin Water, Shimada et al., 2005), and the water in the layer above the temperature minimum is thought to be a mixture of this POW with sea-ice melt and riverine outflow. To determine the fractions (f) of the three different source waters — POW, sea-ice melt (SIM), and riverine outflow (RRO) — in the upper-layer waters of the Chukchi Sea and the Canada Basin, we used the relationship between salinity and TA and the following mass balance equations.

$$\mathrm{TA} = f_{\mathrm{POW}} \cdot \mathrm{TA}_{\mathrm{POW}} + f_{\mathrm{SIM}} \cdot \mathrm{TA}_{\mathrm{SIM}} + f_{\mathrm{RRO}} \cdot \mathrm{TA}_{\mathrm{RRO}} \qquad (7)$$

$$S = f_{\mathrm{POW}} \cdot S_{\mathrm{POW}} + f_{\mathrm{SIM}} \cdot S_{\mathrm{SIM}} + f_{\mathrm{RRO}} \cdot S_{\mathrm{RRO}} \qquad (8)$$

$$1 = f_{\mathrm{POW}} + f_{\mathrm{SIM}} + f_{\mathrm{RRO}} \qquad (9)$$

We chose the data of TA and S from 38 sampling layers/locations in the temperature minimum layer where $T < -1.5$ °C in the Chukchi Sea and the Canada Basin during the cruise, and defined their means (2264.2 ± 12.6 μmol kg^{-1} and 32.89 ± 0.22) as the values of $\mathrm{TA}_{\mathrm{POW}}$ and S_{POW}, respectively (Fig. 1).

There are several studies of TA of riverine outflow in the Arctic. Cooper et al. (2008) directly measured TA in six major rivers in the Arctic: they concluded that flow-weighted average of TA of these six rivers was 1048 μmol kg^{-1}. Yamamoto-Kawai et al. (2009) made linear regression analysis of salinity and TA, and reported that the intercept ($S = 0$) was

793 μmol kg^{-1} for the whole Canada Basin. Data of TA and salinity taken during our cruise indicate that the upper limit of distribution in salinity-TA plots (Fig. 2) is consistent with the line extended to this intercept deduced by Yamamoto-Kawai et al. (2009); consequently, we regarded this value as TA_{RRO}. In consideration of the spatial and temporal fluctuation of riverine TA, we assumed that the uncertainty of TA_{RRO} is ±100 μmol kg^{-1} (Yamamoto-Kawai et al., 2005). Accordingly, the estimated errors of f_{SIM} and f_{RRO} are as large as ±0.02.

Conversely, values of S_{SIM} and TA_{SIM} so far reported fall within a relatively narrow range. We applied $S_{SIM} = 5$ and $TA_{SIM} = 349$ μmol kg^{-1} following Fransson et al. (2009). Differences in f_{SIM} and f_{RRO} are not larger than ±0.008 when applying other values suggested by Anderson et al. (2004) ($S_{SIM} = 4$, $TA_{SIM} = 263$ μmol kg^{-1}). Cumulative error in f_{SIM} and f_{RRO} associated with the selection of the end-member salinity and TA are within ±0.03. As shown in Fig. 2, *S*–TA plots for the Chukchi Sea and Canada Basin fall among the three *S*–TA end-members of POW, SIM, and RRO. Surface water in the Chukchi Sea and Canada Basin consists mainly of POW, but includes sizable f_{SIM} up to 0.16 and f_{RRO} up to 0.18.

4~~3~~. Results and Discussion

~~3.1. Mixing ratio of Pacific-origin, ice-melt, and riverine waters~~

~~In the western Arctic Ocean, the water at the temperature minimum layer (~150 dbar) is known to originate in the North Pacific and be advected into the Arctic through the Bering Strait (POW: Pacific Origin Water, Shimada et al., 2005), and the water in the layer above the temperature minimum is thought to be a mixture of this POW with sea-ice melt and riverine outflow. To determine the fractions (*f*) of the three different source waters — POW, sea-ice melt (SIM), and riverine outflow (RRO) — in the upper-layer waters of the Chukchi Sea and the Canada Basin, we used the relationship between salinity and TA and the following mass balance equations.~~

~~$TA = f_{POW} \cdot TA_{POW} + f_{SIM} \cdot TA_{SIM} + f_{RRO} \cdot TA_{RRO}$ (5)~~

~~$S = f_{POW} \cdot S_{POW} + f_{SIM} \cdot S_{SIM} + f_{RRO} \cdot S_{RRO}$ (6)~~

~~$1 = f_{POW} + f_{SIM} + f_{RRO}$ (7)~~

~~We chose the data of TA and *S* from 38 sampling layers/locations in the temperature minimum layer where $T < -1.5$ °C in the Chukchi Sea and the Canada Basin during the cruise, and defined their means (2264.2 ± 12.6 μmol kg^{-1} and 32.89 ± 0.22) as the values of TA_{POW} and S_{POW}, respectively (Fig. 1).~~

~~There are several studies of TA of riverine outflow in the Arctic. Cooper et al. (2008) directly measured TA in six major rivers in the Arctic: they concluded that flow-weighted average of TA of these six rivers was 1048 μmol kg^{-1}. Yamamoto-Kawai et al. (2009) made linear regression analysis of salinity and TA, and reported that the intercept ($S = 0$) was 793 μmol kg^{-1} for the whole Canada Basin. Data of TA and salinity taken during our cruise indicate that the upper limit of distribution in salinity-TA plots (Fig. 2) is consistent with the line extended to this intercept deduced by Yamamoto-Kawai et al. (2009); consequently, we regarded this value as TA_{RRO}. In consideration of the spatial and temporal fluctuation of riverine TA, we~~

~~assumed that the uncertainty of TARRO is ±100 μmol kg^{-1} (Yamamoto-Kawai et al., 2005). Accordingly, the estimated errors of f_{SIM} and f_{RRO} are as large as ±0.02.~~

~~Conversely, values of S_{SIM} and $\mathrm{TA}_{\mathrm{SIM}}$ so far reported fall within a relatively narrow range. We applied $S_{\mathrm{SIM}} = 5$ and $\mathrm{TA}_{\mathrm{SIM}} = 349$ μmol kg^{-1} following Fransson et al. (2009). Differences in f_{SIM} and f_{RRO} are not larger than ±0.008 when applying other values suggested by Anderson et al. (2004) ($S_{\mathrm{SIM}} = 4$, $\mathrm{TA}_{\mathrm{SIM}} = 263$ μmol kg^{-1}). Cumulative error in f_{SIM} and f_{RRO} associated with the selection of the end-member salinity and TA are within ±0.03. As shown in Fig. 2, S–TA plots for the Chukchi Sea and Canada Basin fall among the three S–TA end-members of POW, SIM, and RRO. Surface water in the Chukchi Sea and Canada Basin consists mainly of POW, but includes sizable f_{SIM} up to 0.16 and f_{RRO} up to 0.18.~~

~~3.2.~~4.1. **Variations in Temperature and Salinity in the Surface Layer**

Cruise MR13-06 occupied a wide area of the Chukchi Sea and the Canada Basin. General variations in surface $p\mathrm{CO_2}^{\mathrm{sea}}$ in these regions have already been well investigated (Bates 2006, Cai et al., 2010). The results from our cruise were not much different from these reports. Therefore, we highlighted below the differences of water mass characteristic and $\mathrm{CO_2}$ dymnamics in these regions. In the period from 4 to 11 September 2013, temperature (SST), salinity (SSS), $p\mathrm{CO_2}^{\mathrm{sea}}$, and DIC in surface water were highly variable in the western Arctic Ocean (Fig. 3), particularly around the continental slope (200 m isodepth in Fig. 3) of the Chukchi Sea. Average $p\mathrm{CO_2}^{\mathrm{air}}$ measured onboard was 385.0 μatm, which is consistent with the value observed at Point Barrow, Alaska (http://ds.data.jma.go.jp/gmd/wdcgg/). According to JRA-55, ~~A~~average U_{10} in the region north of 70°N was 4-5~~7.2~~ m s^{-1} ~~during the cruise~~in September 2013.

Variation in SST and SSS on the cruise track was abrupt rather than gradual (Fig. 3a and 3b). Therefore, we defined three subregions; (1) Barrow Coastal Water (BCW), (2) Canada Basin Water (CBW) and (3) Chukchi Sea Water (CSW). ~~depending on SST and SSS as follows. (1) Barrow Coastal Water (BCW) was relatively warm and fresh (SST > 2 °C, SSS < 30.5). (2) Canada Basin Water (CBW) was cold and fresh (SST < 2 °C, SSS < 28). (3) Chukchi Sea Water (CSW) was saline (SSS > 28).~~ The boundary between BCW and CBW was ~~located~~ 2°C isotherm at 72.5°N, 154.8°W. ~~That between~~ CBW and CSW ~~was~~ were separated by 28 psu isohaline at 73.3°N, 168.3°W (Fig. 3c).

The fraction of freshwater had distinct spatial variations among the three subregions (Fig. 3d and 3e; summarized in Table 1). Low salinity in BCW was mainly due to riverine outflow: in this subregion, f_{RRO} was as large as 0.18, presumably because the Alaskan coastal current which flows northward along the Alaskan coast toward Point Barrow contains a considerable fraction of Yukon River outflow (Steele et al., 2004). In contrast, the lower salinity in the CBW was primarily due to the input of meltwater from sea ice, although it also contained significant riverine outflow. In the northernmost region of the Canada Basin visited during the cruise (north of 74°N), f_{SIM} was as large as 0.16, whereas f_{RRO} was no more than 0.10 and was almost always lower than f_{SIM}. CSW was largely composed of Pacific water and rarely contained riverine outflow as it flowed directly from the Bering Strait.

~~3.3.~~ 4.2. Variations in carbonate chemistry in the Surface Layer

Remarkable differences in pCO_2^{sea}, DIC, and TA were observed among the three subregions (Table 1, Fig. 3f, g, and h). We attributed the low DIC/TA ratio and the ~~resulting~~ low pCO_2^{sea} (< 200 µatm) in CSW to the massive biological activity there in early summer. In this region, net primary production decreases pCO_2^{sea} to 200 µatm or less in early summer (Bates 2006). According to analyses of satellite imagery ~~(Behrenfeld and Falkowski, 1997)~~, net primary productivity (NPP) in July 2013 was as high as 1000 mgC m^{-2} day^{-1} in the majority of the Chukchi Sea. Even though NPP had decreased to ~500 mgC m^{-2} day^{-1} in September 2013 during our measurements, pCO_2^{sea} had been notably lower than pCO_2^{air} for months after the massive primary production in early summer.~~,~~ This was because ~~of relatively slow gas~~ net CO_2 exchange with the atmosphere toward CO2 saturation in surface layer was still in progress. Under typical summer conditions (T = 3 °C, S = 32, DIC = 2000 µmol kg^{-1}, TA = 2220 µmol kg^{-1}, mixed layer depth = 15 m, and U_{10} = 5.0 m s^{-1}), ~~:~~ $\tau_{1/2}$~~the half-life of CO_2 gas exchange, *i.e.*, the time required to reduce ΔpCO_2 by half,~~ ~~was~~ is considered to be ~~about 90~~longer than 100 days ~~under typical summer conditions (T = 3 °C, S = 32, TA = 2220 µmol kg^{-1}, mixed layer depth = 15 m, and U_{10} = 7.2 m s^{-1})~~.

The DIC/TA ratio in CBW was higher than that in CSW (Table 1). The value of pCO_2^{sea} in CBW ranged from 300 to 360 µatm (Fig. 3f). Although the level of pCO_2^{sea} in CBW was still lower than the pCO_2^{air} (385 µatm), it was much higher than that in CSW. The primary cause of the pCO_2^{sea} being nearly as high as pCO_2^{air} is that the addition of meltwater to the surface layer shoals the mixed layer (Cai et al., 2010; Else et al., 2013), thereby reducing the time for surface water to reach air–sea CO_2 equilibrium. An additional cause of higher pCO_2^{sea} in the high f_{SIM} region is probably low net primary production, because the concentrations of nutrients in meltwater are low; e.g., Lee et al. (2012) reported that the concentration of nitrate in a melt pond being formed on the top of sea ice in the Canada Basin was low (< 0.5 µM), and that the low nitrate concentration limited biological production in the pond. Our results corroborate previous reports by Cai et al. (2010) and Else et al. (2013) that the overspreading of the surface layer by sea-ice melt inhibits CO_2 uptake by the ocean. ~~High~~Near equilibrium pCO_2^{sea} conditions after seasonal sea-ice retreat is likely to be common in the Canada Basin. The impact of sea-ice melt itself on pCO_2^{sea} was difficult to resolve only from our observations. Bates et al. (2014) found both basic (i.e., DIC/TA < 1) and relatively acidic (i.e., DIC/TA > 1) melt ponds in the Canada Basin. To study the impact of meltwater on carbonate chemistry, direct sampling of sea ice into gastight bags (Fransson et al., 2013) will be required.

In BCW, pCO_2~~sea~~^{sea} was about 270 µatm on average, between that in CSW and CBW (Fig. 3f). The fraction of freshwater indicates that surface freshening in BCW is mainly caused by riverine outflow (f_{RRO} = 0.11) rather than sea-ice melt (f_{SIM} = 0.08). Riverine outflow had a higher TA/S ratio than sea-ice melt (Fig. 2). It also has larger content of DIC (Ulfsbo et al., 2014). In our measurements, surface chlorophyll *a* was higher in BCW (0.4 to 2.0 mg dm^{-3}) than in CBW (0.1 to 0.3 mg dm^{-3}), implying that biological drawdown of DIC was greater in BCW. Consequently, both DIC/TA and pCO_2^{sea} in BCW were lower than those in CBW. ~~Reduction in CO_2 absorption capacity by riverine discharge was not as large as that by sea-ice melt.~~ At the time of our observation, BCW still could absorb more CO_2 from the atmosphere than offshore CBW.

This is an important finding, because river water inflow into the Arctic Ocean is considered highly likely to increase with climate change (McClelland et al., 2006; Déry et al., 2009).

~~3.4.~~ 4.3. Variations in the Water Column

Water properties ~~among the three subregions~~ differed not only in the surface but also in the water column among these three. T-S diagrams obtained by CTD for each subregion are shown in Fig. 4. The surface around Point Barrow was fresh and warm; ~~with depth~~as depth increases, the water column gradually cooled to the coldest water around $S = 33$ (Fig. 4a). A similar decrease in temperature from near surface to bottom was observed in the Chukchi Sea (Fig. 4b). In contrast, the water column in the Canada Basin was more complex, with a number of temperature maxima and minima (Fig. 4c). Jackson et al. (2010) classified the water column in the Canada Basin from the top to the bottom into a surface mixed layer, a near surface temperature maximum (NSTM), a remnant of the Winter Mixed Layer (rWML), Pacific Summer Water (PSW), and Pacific Winter Water (PWW). The surface mixed layer had the lowest salinity ($S < 27$) because almost all sea-ice melt is trapped in this layer during summer. The NSTM is separated from the surface mixed layer by stratification and warmed by the input of solar radiation. The depths of NSTM ranged between 15 and 26 m during our observations. Below the NSTM, the rWML corresponded to the temperature minimum (T ≈~~=~~ –1 ℃, S ≈~~=~~ 29.3), which was formed in the Canada Basin during the previous winter. Another temperature maximum around $S = 30.5$ corresponded to PSW, which was advected and modified in the Chukchi Sea during summer. The lowest temperature observed was ~~PWW~~ near the freezing point in PWW at ~~and around~~around $S = 33.1$.

Temperature and salinity were frequently ~~observed~~ measured along the cruise track by CTD and XCTD sensors. Water ~~C~~column profiles ~~included~~ showed a distinct halocline from 10 to 20 dbar in BCW and CBW (Fig. 5a and 5b). In these two subregions, the ~~salinity~~ difference in salinity ~~gradient from~~between above~~ the halocline~~ and~~to~~ below the halocline ~~it~~ was up to 2. Unlike the other two subregions, ~~In CSW, the~~ thermocline was more prominent than halocline~~, although not as clear as in the other two subregions, was at almost the same depth~~ in CSW. Column variation of f_{SIM} and f_{RRO} indicate that both sea-ice meltwater and river outflow greatly ~~affected~~contributed to the formation of the halocline (Fig. 5c and 5d). In the Canada Basin, f_{SIM} was as high as 0.12 ± 0.01 (± standard deviation) in the top layer down to 10 dbar, but decreased abruptly with depth to practically zero (0.01 ± 0.01) in the 29–50 dbar layer. ~~In contrast~~Likewise, f_{RRO} was also quite high (0.09 ± 0.01) in the top layer down to 10 dbar and decreased gradually to 0.06 ± 0.02 in the 29–50 dbar layer. This vertical structure indicates that the input of sea-ice melt occurred shortly before the measurement (at least, in summer 2013) and contributed to the formation of a discrete layer in the surface over the main water mass in the Canada Basin, whereas river outflow had undergone vertical mixing in the course of advection before it reached the Canada Basin.

Among these three subregions, differences were also evident in column $p\mathrm{CO}_2^{\mathrm{sea.}}$ In the upper layer (above 10 dbar) of CSW and BCW, average $p\mathrm{CO}_2^{\mathrm{sea}}$ was 195 ± 11 µatm and 258 ± 14 µatm, respectively. As mentioned in section ~~3~~4.2, these low $p\mathrm{CO}_2^{\mathrm{sea}}$ values were the result of net primary production. In these subregions, $p\mathrm{CO}_2^{\mathrm{sea}}$ increased with depth below the halocline. The water column profile of AOU indicates that the increase in $p\mathrm{CO_2}^{\mathrm{sea}}$ was due to the input of CO_2 associated with the degradation of organic matter (Fig. 5e and 5f).

Unlike the water column profiles of $p\mathrm{CO_2}^{\mathrm{sea}}$ and AOU in CSW and BCW, those in CBW were distinctive in that they had subsurface minima. In the top 10 dbar of CBW, $p\mathrm{CO_2}^{\mathrm{sea}}$ reached 322 ± 20 µatm, a value still lower than $p\mathrm{CO_2}^{\mathrm{air}}$ (~385 µatm) but the highest among the three subregions. However, $p\mathrm{CO_2}^{\mathrm{sea}}$ decreased with depth below the halocline and reached 271 ± 31 µatm in the range of 29.~~4~~ 3 $< S <$ 31.3 (30 to 50 dbar layer; Fig. 5e and 6a). Below the halocline in CBW, AOU was significantly ~~largely~~ negative ~~(~~~ (< –~~40~~ 20 µmol kg^{-1}) like that in the CSW where net primary production was large (Fig. 5f and 6b).

Subsurface ~~maxima~~ maximum of chlorophyll *a* and dissolved oxygen have also been found in the Canadian Archipelago (Martin et al., 2010). Here, our frequent observations facilitated classification of the water masses and their origins; this in turn explains the biological production in the subsurface layer of the Canada Basin. According to the salinity–AOU profile (Figure 6b) in the Canada Basin, AOU was largely negative (< -20 µmol kg^{-1}) in the salinity range of 28 to 31.5 that corresponds to NSTM, rWML and PSW. NSTW and rWML were formed in the Canada Basin. Nitrates were almost depleted (< 0.2 µmol kg^{-1}) in these two layers during our observations (Figure 6c). Even in spring, concentration of nitrate was low (< 2 µmol kg^{-1}) in surface water of the Canada Basin (Codispoti et al., 2005). Sunlight surely reaches the 50 m depth in the Canada Basin although it is not strong (Jackson et al., 2010). Negative AOU in NSTM and rWML indicated the large biological production utilizing the nutrients and the sunlight. Excess oxygen produced by the biological production remained in subsurface as it was isolated from surface by strong halocline. Results of our measurements also showed that significant nutrients remained in PSW where $S > 29.3$ (Figure 6c). Oversaturation of oxygen in PSW was due to the remnant of massive biological production in early summer and/or the production undersea during advection from the Chukchi Sea to the Canada Basin.

To compare the water properties among layers, we calculated preformed $\mathrm{nDIC_{32}}$ as defined by the following equation.

$$\text{Preformed nDIC}_{32} = \frac{\text{DIC} - \text{AOU} \times r_{C:O}}{S} \times 32 \qquad (10)$$

Here, $r_{C:O}$ denotes stoichiometric ratio of DIC to AOU being set to 117/170 (Anderson and Sarminento, 1994). As shown in Fig. 6d, preformed $\mathrm{nDIC_{32}}$ was almost constant and the highest in the water column from surface to $S = 29.3$. This indicates that the water above $S = 29.3$ had the same origin in the Canada Basin. There was no clear minimum of $p\mathrm{CO_2}^{\mathrm{sea}}$ in NSTM and rWML in spite of the negative AOU and biological production. This was because NSTM and rWML had high preformed DIC and biological production was limited by low nutrients. Preformed $\mathrm{nDIC_{32}}$ in the salinity range of 29.3 to 33.1 was lower than that of surface water by about 100 µmol kg^{-1}. This water with this salinity range corresponds to PSW and PWW that have their origins in the Chukchi Sea. Consequently, $p\mathrm{CO_2}^{\mathrm{sea}}$ minimum in subsurface in the Canada Basin was attributable not only to large biological drawdown of DIC but also to lower DIC in PSW as compared with Canada Basin origin water lying above.~~According to the salinity–AOU profile (Figure 6b) in the Canada Basin, AOU was negative (i.e.,~~

~~oxygen was saturated) in the range of $29.5 < S < 31.0$ corresponding rWML and PSW. These water types were present in the 30–50 m depth layer (Fig. 5b). A column profile of photosynthetically active radiation in the Canada Basin shows that, although not strong, sunlight surely reaches the 50 m depth (Jackson et al., 2010); this sunlight fueled net primary production in the rWML with nutrients entrained during winter mixing. Oxygen supersaturation was greater in PSW than in rWML, even though PSW was deeper, probably because of massive primary production in the Chukchi Sea; the PSW there very likely subducted and advected into the Canada Basin before releasing all its excess oxygen to the atmosphere.~~

~~3.5.~~ 4.4. Future direction of hidden CO_2 sink in the Canada Basin

~~Predictions of the effects of a~~How the long-term retreat of sea ice effect on the air–sea CO_2 flux in the Arctic Ocean ~~are~~ is a matter of con~~tradictory~~troversy. ~~For example,~~ Manizza et al. (2013) argued that increasing SST will enhance biological primary production and drawdown of CO_2 in seawater. Laruelle et al. (2014) asserted that larger ice-free areas and longer ice-free periods will provide greater occasion for oceanic CO_2 uptake. In contrast, Cai et al. (2010) and Else et al. (2013) insisted that the increase in sea-ice melt results in the formation of thin surface mixed layers and limits further uptake of ~~atmospheric~~ CO_2 from the atmosphere by this layer.

As a result of our observations that a subsurface minimum of pCO_2^{sea} existed in the Canada Basin, it is necessary to study whether the surface mixed layer there will deepen under a warming climate. If the surface ~~seawater~~ layer is stirred by strong wind and mixed with~~,~~ the subsurface low pCO_2^{sea} layer, ~~that mixes with~~ the surface will act as a further CO_2 sink. Several reports indicate that the ~~deepening of the surface mixed layer by~~ strong wind associated with the passage of low pressure systems deepens the surface mixed layer and has impacts on the ~~and their~~ biogeochemistry~~cal impacts~~ (Wada et al., 2011; Rumyantseva et al., 2015). Simmonds and Keay (2009) reported that the strength of cyclones in the Arctic Ocean is increasing with the long-term reduction of sea-ice cover. However, we ~~must~~ also have to consider the strength of stratification in the Canada Basin. In a comprehensive analysis of mixed layer depth in the Arctic Ocean, Peralta-Ferriz et al. (2015) found a significant positive correlation ~~(4.6 ± 0.8 m per m sec^{-1})~~ between the mixed layer depth and the maximum wind speed in the preceding 5 days (4.6 ± 0.8 m per m sec^{-1}) in the case that the ~~of~~ differences in density between the mixed layer and 20 m below ~~it~~ ($\Delta\rho$) is ~~being~~ smaller than 0.5 kg m^{-3}. However, ~~I~~in the case of $\Delta\rho > 0.5$ kg m^{-3}, deepening of the mixed layer is much less sensitive to~~accompanying~~ the increase in wind speed ~~was almost zero~~ (0.77 ± 0.52 m per m sec^{-1}). In our observations, $\Delta\rho$ exceeded 2.0 kg m^{-3} at all CTD stations in the Canada Basin (Fig. 4c). Hence, we ~~think~~suggest that additional CO_2 uptake in the Canada Basin by wind mixing is unlikely because stratification was strong even in 2013 and will be further strengthened by ~~further~~the additional input of sea-ice melt in the future.

Climate change also affects the subsurface layer in the Canada Basin, where low pCO_2^{sea} is caused by net primary production. McLaughlin and Carmack (2010) reported that increase in sea-ice melt and the strengthening of Ekman pumping deepened the nutricline and the depth of chlorophyll maximum in the Canada Basin. Nishino et al. (2013) also observed decreases in nitrate and chlorophyll in the 0 to 50 m depth layer in the Canada Basin during 2002–2010; they attributed these decreases to the decrease in inflow of nutrient-rich water from the East Siberia Sea. In any case, biological production below the halocline of the Canada Basin is likely to decrease in the long term. In this regard, it seems unlikely that the subsurface low $p\mathrm{CO}_2^{\mathrm{sea}}$ layer in the Canada Basin will act as another CO_2 sink.

~~4~~5. Conclusions

A wide range of surface $p\mathrm{CO}_2^{\mathrm{sea}}$ was observed in the western Arctic Ocean in September 2013. The value was as low as 180 μatm in the Chukchi Sea where biological activity was high in early summer. In contrast, $p\mathrm{CO}_2^{\mathrm{sea}}$ in the Canada Basin in September reached 360 μatm, ~~almost equivalent~~the value comparable to $p\mathrm{CO}_2^{\mathrm{air}}$. Based on ~~our use of~~the relationship between ~~-~~salinity and TA~~ to identify the fraction of freshwater~~, we attributed the low salinity water in the Canada Basin to the input of sea-ice melt. Large input of oligotrophic sea-ice melt not only inhibits biological activity, but also facilitates to form~~s~~ a thin surface mixed layer that is easier~~ly~~ to reach~~es~~ equilibrium with respect to the atmospheric CO_2. In the area where mixing with riverine output was more dominant than with sea-ice melt, the increase in $p\mathrm{CO}_2^{\mathrm{sea}}$ was indistinct due to the input of riverine nutrients and TA. ~~Although both meltwater and river water are freshwater, the effects of riverine output differed from those of sea-ice melt.~~

In the Canada Basin $p\mathrm{CO}_2^{\mathrm{sea}}$ was the lowest (~250 μatm) under the surface mixed layer below a strong halocline (difference in density~~ gradient~~ ~~>~~ is larger than 2.0 kg m^{-3}). ~~was formed under the surface mixed layer, where $p\mathrm{CO}_2^{\mathrm{sea}}$ was the lowest (~250 μatm); this~~This differs from other regions where ~~$p\mathrm{CO}_2^{\mathrm{sea}}$ was~~the lowest $p\mathrm{CO}_2^{\mathrm{sea}}$ was observed in ~~at~~ the surface. This subsurface $p\mathrm{CO}_2^{\mathrm{sea}}$ minimum correspond~~ed~~s to~~ rWML and~~ PSW and ~~is~~ is attributable to the lager net primary production and originally lower DIC of PSW compared to those water of Canada Basin-origin. The subsurface low $p\mathrm{CO}_2^{\mathrm{sea}}$ layer in the Canada Basin has a potential to absorb ~~atmospheric~~ CO_2 from the atmosphere in case it is ~~transported to~~mixed with the surface by ~~vertical mixing~~a strong turbulance. However, such an increase of CO_2 absorption~~sink~~ is unlikely because this stratification is strong enough to resist vertical mixing by wind. Additionally, long-term observations in the Canada Basin suggest that subsurface biological activity has been declining in recent decades.

Our observations ~~revealed~~ could reveal only a part of the complex carbon cycle in the Arctic Ocean. The subsurface $p\mathrm{CO}_2^{\mathrm{sea}}$ minimum is ~~peculiar~~ specific to the Canada Basin~~,~~ where circulation of ~~a complicated~~ waters generates a complicated water column structure~~ exists~~; the~~se~~ results here are unlikely to be applicable to the entire Arctic Ocean. In the changing Arctic Ocean, although these subregional variations and processes are essential for ~~accurate~~ better projections of the future carbon cycle, they are not adequately reflected in current models. The areas we can ~~O~~observe~~able areas~~ in the Arctic Ocean are expected to expand along with the long-term sea-ice retreat. Comprehensive observations are essential especially in such areas because sea-ice melt may cause other ~~unknown~~ effects that are unknown to date.

References

Anderson, L. G., Jutterström, S., Kaltin, S., Jones, E. P., and Björk, G.–: Variability in river runoff distribution in the Eurasian Basin of the Arctic Ocean, J. Geophys. Res., 109, C01016, doi:10.1029/2003JC001773, 2004.

Anderson, L. and Sarmiento, J.: Redfield ratios of remineralization determined by nutrient data analysis, Global Biogeochemcal Cycles, 8, 65-80, 1994.

Aoyama, M. and Hydes, D. J.: How do we improve the comparability of nutrient measurements?, in: Comparability of Nutrients in the World's Ocean, edited by: Aoyama, M., Dickson, A. G., Hydes, D. J., Murata, A., Oh, J. R., Roose, P., and Woodward E. M. S., Mother Tank, Tsukuba, Japan, 1-10, 2010.

Bates, N. R.: Air-sea CO_2 fluxes and the continental shelf pump of carbon in the Chukchi Sea adjacent to the Arctic Ocean, J. Geophys. Res., 111, C10013, doi:10.1029/2005JC003083, 2006.

Bates, N. R. and Mathis, J. T.: The Arctic Ocean marine carbon cycle: Evaluation of air-sea CO_2 exchanges, ocean acidification impacts and potential feedbacks, Biogeosciences, 6, 2433–2459, doi:10.5194/bg-6-2433-2009, 2009.

Bates, N. R., Garley, R., Frey, K. E., Shake, K. L., and Mathis, J. T.: Sea-ice melt CO_2–carbonate chemistry in the western Arctic Ocean: meltwater contributions to air–sea CO_2 gas exchange, mixed-layer properties and rates of net community production under sea ice, Biogeosciences, 11, 6769-6789, doi:10.5194/bg-11-6769-2014, 2014.

Behrenfeld, M. J. and Falkowski, P. G.: A consumers guide to phytoplankton primary production models, Limnol. Oceanogr., 42(7), 1479–1491, 1997.

Cai, W.-J., Chen, L., Chen, B., Gao, Z., Lee, S.H., Chen, J., Pierrot, D., Sullivan, K., Wang, Y., Hu, X., Huang, W.-J., Zhang, Y., Xu, S., Murata, A., Grebmeier, J. M., Jones, E. P., and Zhang, H.: Decrease in the CO_2 uptake capacity in an ice-free Arctic Ocean basin, Science, 329, 556–559, doi:10.1126/science.1189338, 2010.

Codispoti, L. A., Flagg, C., Kelly, V., and Swift, J. H.: Hydrographic conditions during the 2002 SBI process experiments, Deep Sea Res., Part II, 52, 3199–3226, doi:10.1016/j.dsr2.2005.10.007, 2005.

Comiso, J.: Large decadal decline of the Arctic multiyear ice cover, J. Clim., 25, 1176–1193, doi:10.1175/JCLI-D-11-00113.1, 2012.

Cooper, L. W., McClelland, J. W., Holmes, R. M., Raymond, P. A. Gibson, J. J., Guay, C. K., and Peterson, B. J.: Flow-weighted values of runoff tracers (δ^{18}O, DOC, Ba, alkalinity) from the six largest Arctic rivers, Geophys. Res. Lett., 35, L18606, doi:10.1029/2008GL035007, 2008.

Déry, S. J., Hernández-Henríquez, M. A., Burford, J. E., and Wood, E. F.: Observational evidence of an intensifying hydrological cycle in northern Canada, Geophys. Res. Lett., 36, L13402, doi:10.1029/2009GL038852, 2009.

Dickson, A.G.: Determination of dissolved oxygen in sea water by Winkler titration, in WHP Operations and Methods. WHP Office Report Woods Hole, Massachusetts, USA, pp. 1–14, 1994.

Dickson, A. G., Sabine, C. L., and Christian, J. R.: Guide to best practices for ocean CO_2 measurements, Sidney, British Columbia, North Pacific Marine Science Organization, PICES Special Publication 3, 2007.

Else, B. G. T., Galley, R. J., Lansard, B., Barder, D. G., Brown, K., Miller, L. A., Mucci, A., Papakyriakou, T. N. Tremblay, J.-É., and Rysgaard, S.: Further observations of a decreasing atmospheric CO_2 uptake capacity in the Canada Basin (Arctic Ocean) due to sea ice loss, Geophys. Res. Lett., 40, 1132–1137, doi:10.1002/grl.50268, 2013.

Fransson, A., Chierici, M., and Nojiri, Y.: New insights into the spatial variability of the surface water carbon dioxide in varying sea ice conditions in the Arctic Ocean, Cont. Shelf Res., 29, 1317–1328, doi:10.1016/j.csr.2009.03.008, 2009.

Fransson, A., Chierici, M., Miller, L. A., Carnat, G., Shadwick, E., Thomas, H., Pineault, S., and Papakyriakou, T. N.: Impact of sea-ice processes on the carbonate system and ocean acidification at the ice-water interface of the Amundsen Gulf, Arctic Ocean, J. Geophys. Res. Oceans, 118, 7001–7023, doi:10.1002/2013JC009164, 2013.

Hydes, D. J., Aoyama, M., Aminot, A., Bakker, K., Becker, S., Coverly, S., Daniel, A., Dickson, A. G., Grosso, O., Kerouel, R., van Ooijen, J., Sato, K., Tanhua, T., Woodward, E. M. S., and Zhang, J. Z.: Determination of dissolved nutrients (N, P, Si) in seawater with high precision and inter-comparability using gas-segmented continuous flow analysers. In The GO-SHIP Repeat Hydrography Manual: A Collection of Expert Reports and guidelines. IOCCP Report No 14, ICPO Publication Series No. 134, version 1, 2010.

~~Hsu, S. A., Meindl, E. A, and Gilhousen, D. B.: Determining the power-law wind-profile exponent under near-neutral stability conditions at sea, J. Appl. Meteorol., 33, 757 – 765, 1994.~~

Jackson, J. M., Carmack, E. C., McLaughlin, F. A., Allen, S. E., and Ingram, R. G.: Identification, characterization, and change of the near-surface temperature maximum in the Canada Basin, 1993–2008, J. Geophys. Res., 115, C05021, doi:10.1029/2009JC005265, 2010.

Kobayashi, S., Ota, Y., Harada, Y., Ebita, A., Moriya, M., Onoda, H., Onogi, Kamahori, H., Kobayashi, C., Endo, H., Miyaoka, K., and Takahashi, K.: The JRA-55 Reanalysis: General specifications and basic characteristics, J. Meteorol. Soc. Jpn., 93, 5–48, doi:10.2151/jmsj.2015-001., 2015.

Laruelle, G. G., Lauerwald, R., Pfeil, B., and Regnier, P.: Regionalized global budget of the CO_2 exchange at the air-water interface in continental shelf seas, Global Biogeochem. Cycles, 28, 1199–1214, doi:10.1002/2014GB004832, 2014.

Lee, S. H., Stockwell, D. A., Joo, H.-M., Son, Y. B., Kang, C.-K., and Whitledge, T. E.: Phytoplankton production from melting ponds on Arctic sea ice, J. Geophys. Res., 117, C04030, doi:10.1029/2011JC007717, 2012.

Le Quéré, C., Andrew, R. M., Canadell, J. G., Sitch, S., Korsbakken, J. I., Peters, G. P., Manning, A. C., Boden, T. A., Tans, P. P., Houghton, R. A., Keeling, R. F., Alin, S., Andrews, O. D., Anthoni, P., Barbero, L., Bopp, L., Chevallier, F., Chini, L. P., Ciais, P., Currie, K., Delire, C., Doney, S. C., Friedlingstein, P., Gkritzalis, T., Harris, I., Hauck, J., Haverd, V., Hoppema, M., Klein Goldewijk, K., Jain, A. K., Kato, E., Körtzinger, A., Landschützer, P., Lefèvre, N., Lenton, A., Lienert, S., Lombardozzi, D., Melton, J. R., Metzl, N., Millero, F., Monteiro, P. M. S., Munro, D. R., Nabel, J. E. M. S., Nakaoka, S.-I., O'Brien, K., Olsen, A., Omar, A. M., Ono, T., Pierrot, D., Poulter, B., Rödenbeck, C., Salisbury, J., Schuster, U., Schwinger, J., Séférian, R., Skjelvan, I., Stocker, B. D., Sutton, A. J., Takahashi, T., Tian, H., Tilbrook, B., van der Laan-Luijkx, I. T., van der Werf, G. R., Viovy, N., Walker, A. P., Wiltshire, A. J., and Zaehle, S.: Global Carbon Budget 2016, Earth Syst. Sci. Data, 8, 605-649, doi:10.5194/essd-8-605-2016, 2016.

Lueker, T. J., Dickson, A. G., and Keeling, C. D.: Ocean pCO_2 calculated from dissolved inorganic carbon, alkalinity, and equations for K_1 and K_2: Validation based on laboratory measurements of CO_2 in gas and seawater in equilibrium, Mar. Chem., 70, 105–119, 2000.

Manizza, M., Follows, M. J., Dutkiewicz, S., Menemenlis, D., Hill, C. N., and Key, R. M.: Changes in the Arctic Ocean CO_2 sink (1996–2007): A regional model analysis, Global Biogeochem. Cycles, 27, 1108–1118, doi:10.1002/2012GB004491, 2013.

Martin, J., Tremblay, J.-É., Gagnon, J., Tremblay, G., Lapoussiére, A., Jose, C., Poulin, M., Gosselin, M., Gratton, Y., and Michel, C.: Prevalence, structure and properties of subsurface chlorophyll maxima in Canadian Arctic waters, Mar. Ecol. Prog. Ser., 412, 69–84, doi:10.3354/meps08666, 2010.

McClelland, J. W., Déry, S. J., Peterson, B. J., Holmes, R. M., and Wood, E. F.: A pan-arctic evaluation of changes in river discharge during the latter half of the 20th century, Geophys. Res. Lett., 33, L06715, doi:10.1029/2006GL025753, 2006.

McLaughlin, F. A. and Carmack, E. C.: Deepening of the nutricline and chlorophyll maximum in the Canada Basin interior, 2003–2009, Geophys. Res. Lett., 37, L24602, doi:10.1029/2010GL045459, 2010.

Midorikawa~~Mirorikawa~~, T., Ishii, M., Nemoto, K., Kamiya, H., Nakadate, A., Masuda, S., Matsueda, H., Nakano, T., and Inoue, H. Y.: Interannual variability of winter oceanic CO_2 and air-sea CO_2 flux in the western North Pacific for 2 decades, J. Geophys. Res., 111, C07S02, doi:10.1029/2005JC003095, 2006.

Nishino, S., Itoh, M., Williams, W. J., and Semiletov, I.: Shoaling of the nutricline with an increase in near-freezing temperature water in the Makarov Basin, J. Geophys. Res. Oceans, 118, 635–649, doi:10.1029/2012JC008234, 2013.

Nishino, S., Kawaguchi, Y., Inoue, J., Hirawake, T., Fujiwara, A., Futsuki, R., Onodera, J., and Aoyama, M.: Nutrient supply and biological response to wind-induced mixing, inertial motion, internal waves, and currents in the northern Chukchi Sea, J. Geophys. Res. Oceans, 120, 1975–1992, doi:10.1002/2014JC010407, 2015.

Parkinson, C. L. and Comiso, J. C.: On the 2012 record low Arctic sea ice cover: Combined impact of preconditioning and an August storm, Geophys. Res. Lett., 40, 1356–1361, doi:10.1002/grl.50349, 2013.

Peralta-Ferriz, C. and Woodgate, R. A.: Seasonal and interannual variability of pan-Arctic surface mixed layer properties from 1979 to 2012 from hydrographic data, and the dominance of stratification for multiyear mixed layer depth shoaling, Prog. Oceanogr., 134, 19–53, doi:10.1016/j.pocean.2014.12.005, 2015.

Pierrot, D., Lewis, E., and Wallace, D. W. R.; : CO2SYS DOS Program Developed for CO2System Calculations. ORNL/CDIAC-105, Carbon Dioxide Information Analysis Center, Oak Ridge National Laboratory, US Department of Energy, Oak Ridge, California, 2006.

Rabe, B., Karcher, M., Kauker, F., Schauer, U., Toole, J. M., Krishfield, R. A., Pisarev, S., Kikuchi, T., and Su, J.: Arctic Ocean basin liquid freshwater storage trend 1992–2012, Geophys. Res. Lett., 41, 961–968, doi:10.1002/2013GL058121, 2014.

Rumyantseva, A., Lucas, N., Rippeth, T., Martin, A, Painter, S. C., Boyd, T. J., and Henson, S.: Ocean nutrient pathways associated with the passage of a storm, Global Biogeochem. Cycles, 29, 1179–1189, doi:10.1002/2015GB005097, 2015.

Rysgaard, S., Glud, R. N., Sejr, M. K., Bendtsen, J., and Christensen, P. B.: Inorganic carbon transport during sea ice growth and decay: A carbon pump in polar seas, J. Geophys. Res., 112, C03016, doi:10.1029/2006JC003572, 2007.

Shimada, K., Itoh, M., Nishino, S., McLaughlin, F., Carmack, E., and Proshutinsky A.: Halocline structure in the Canada Basin of the Arctic Ocean, Geophys. Res. Lett., 32, L03605, doi:10.1029/2004GL021358, 2005.

Simmonds, I., and Keay, K.: Extraordinary September Arctic sea ice reductions and their relationships with storm behavior over 1979–2008, Geophys. Res. Lett., 36, L19715, doi:10.1029/2009GL039810, 2009.

Steele, M., Morison, J., Ermold, W., Rigor, I., Ortmeyer, M., and Shimada, K.: Circulation of summer Pacific halocline water in the Arctic Ocean, J. Geophys. Res., 109, C02027, doi:10.1029/2003JC002009, 2004.

Stroeve, J. C., Kattsov V., Barrett, A., Serreze, M., Pavlova, T., Holland, M., and Meiner, W. N.: Trends in Arctic sea ice extent from CMIP5, CMIP3 and observations, Geophys. Res. Lett., 39, L16502, doi:10.1029/2012GL052676, 2012a.

Stroeve, J. C., Serreze, M. C., Holland, M. M., Kay, J. E., Malanik, J., and Barrett, A. P.: The Arctic's rapidly shrinking sea ice cover: A research synthesis, Clim. Change, 110, 1005–1027, doi:10.1007/s10584-011-0101-1, 2012b.

Takahashi, T., Sutherland, S. C., Wanninkhof, R., Sweeney, C., Feely, R. A., Chipman, D. W., Hales, B., Friederich, G., Chavez, F., Sabine, C., Watson, A., Bakker, D. C. E., Schuster, U., Metzl, N., Yoshikawa-Inoue, H., Ishii, M., Midorikawa, T., Nojiri, Y., Kortzinger, A., Steinhoff, T., Hoppema, M., Olafsson, J., Arnarson, T. S., Tilbrook, B., Johannessen, T., Olsen, A., Bellerby, R., Wong, C. S., Delille, B., Bates, N. R., and de Baar, H. J. W: Climatological mean and decadal change in surface ocean $p\mathrm{CO_2}$, and net sea-air $\mathrm{CO_2}$ flux over the global oceans, Deep Sea Res., Part II, 56(8–10), 554–577, doi:10.1016/j.dsr2.2008.12.009, 2009.

Ulfsbo, A., Cassar, N., Korhonen, M., van Heuven, S., Hoppema, M., Kattner, G., and Anderson, L. G.: Late summer net community production in the central Arctic Ocean using multiple approaches, Global Biogeochem. Cycles, 28, 1129–1148, doi:10.1002/2014GB004833, 2014.

Wada, A., Midorikawa, T., Ishii, M., and Motoi, T.: Carbon system changes in the East China Sea induced by Typhoons Tina and Winnie in 1997, J. Geophys. Res., 116, C07014, doi:10.1029/2010JC006701, 2011.

Wanninkhof, R.: Relationship between wind speed and gas exchange over the ocean revisited, Limnol. Oceanogr-Meth., 12, 351–362, 2014.

~~Wanninkhof, R. H.: Relationship between wind speed and gas exchange over the ocean, J. Geophys. Res., 97, 7373–7382, 1992.~~

Weiss, R. F.: Carbon dioxide in water and seawater: The solubility of a non-ideal gas, Mar. Chem., 2, 203–215, 1974.

Yamamoto-Kawai, M., Tanaka, N., and Pivovarov, S.: Freshwater and brine behaviors in the Arctic Ocean deduced from historical data of δ^{18}O and alkalinity (1929–2002 A.D.), J. Geophys. Res., 110, C10003, doi:10.1029/2004JC002793, 2005.

Yamamoto-Kawai, M., McLaughlin, F. A., Carmack, E. C., Nishino, S. Shimada, K., and Kurita, N.: Surface freshening of the Canada Basin, 2003–2007: River runoff versus sea ice meltwater, J. Geophys. Res., 114, C00A05, doi:10.1029/2008JC005000, 2009.

Yao, W. S. and Byrne, R. H.: Simplified seawater alkalinity analysis: Use of linear array spectrometers, Deep Sea Res., Part I, 45(8), 1383–1392, doi:10.1016/S0967-0637(98)00018-1, 1998.

Zhao, C. L., and Tans, P. P.: Estimating uncertainty of the WMO mole fraction scale for carbon dioxide in air, J. Geophys. Res., 111, D08509, doi:10.1029/2005JD006003, 2006.

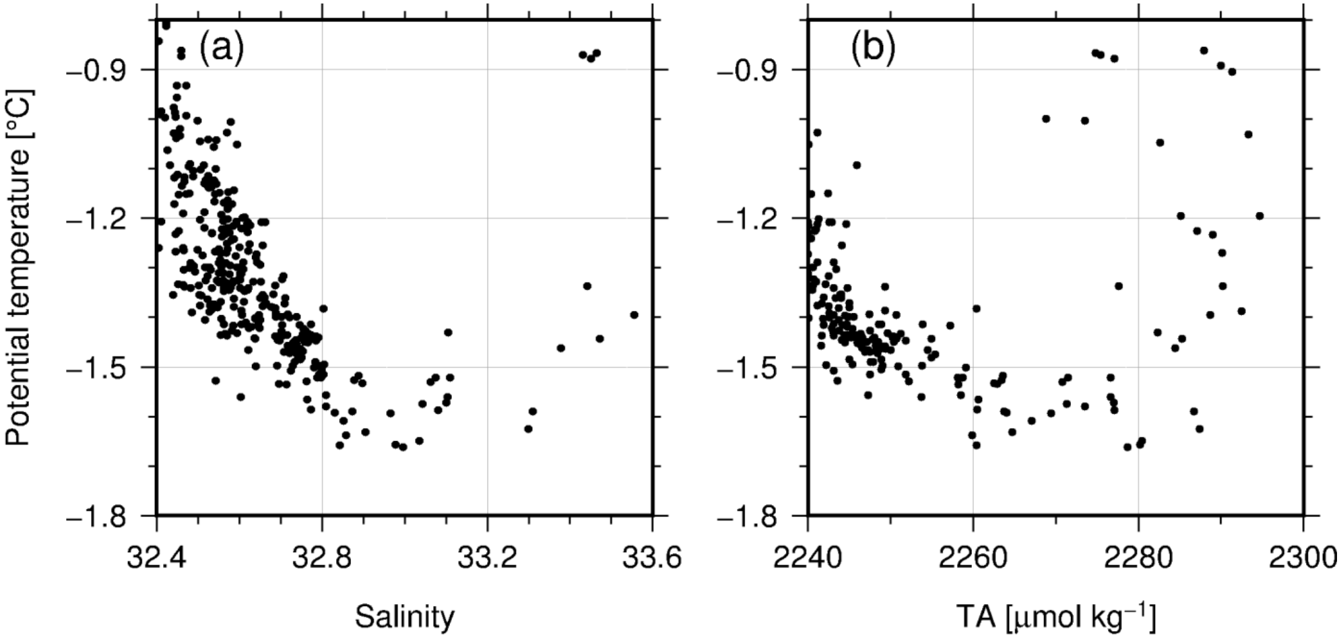

Figure 1: Water properties around the temperature minimum layer in the Chukchi Sea and the Canada Basin in samples collected during cruise MR13-06 from 3 September to 1 October 2013. Potential temperature versus (a) salinity and (b) total alkalinity (TA).

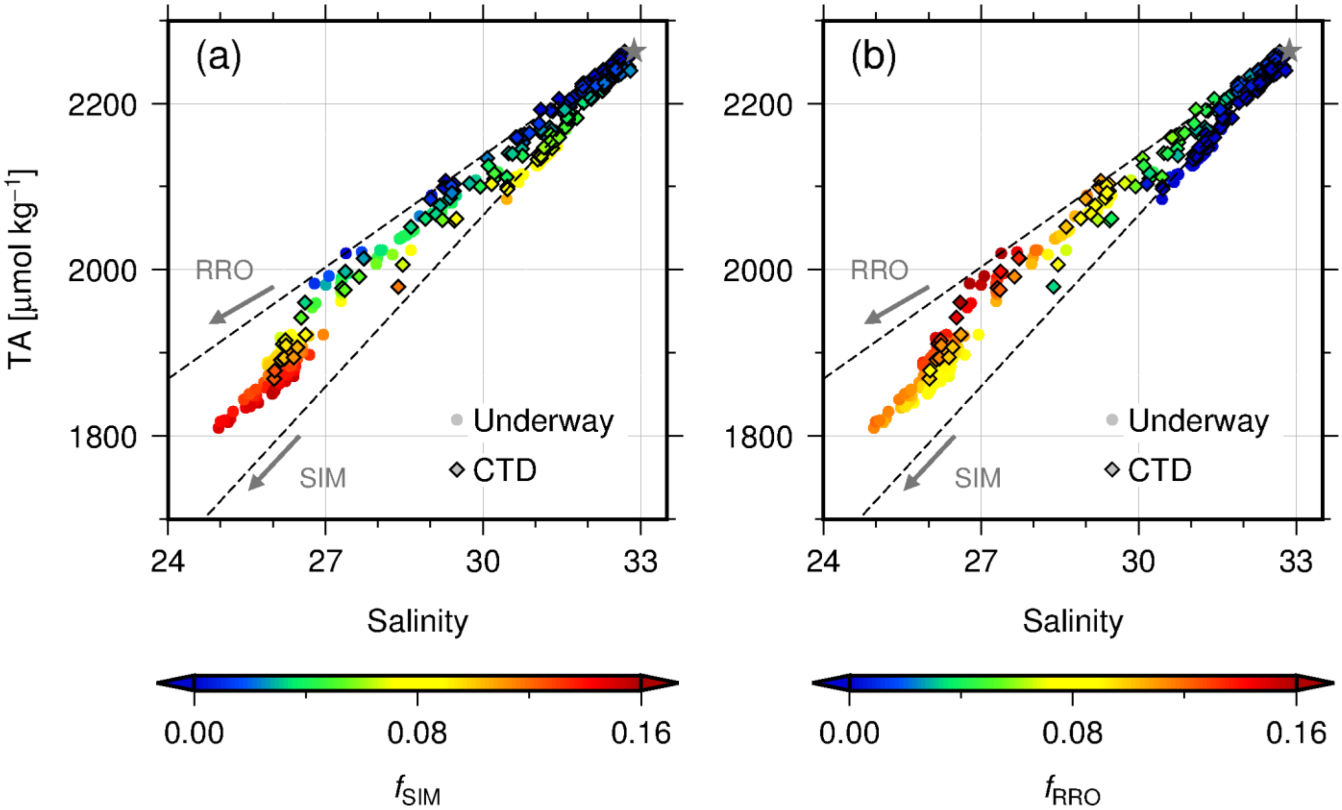

Figure 2: TA versus salinity in the western Arctic Ocean above the temperature minimum layer from 4 to 11 September 2013 color coded for (a) the fraction of sea-ice melt (f_{SIM}) and (b) the fraction of riverine outflow (f_{RRO}). Circles and diamonds denote surface water and CTD samples, respectively. Star denotes the salinity and TA of Pacific origin water (POW: S = 32.89 and TA = 2264.2 μmol kg^{-1}). Broken lines extend to the two endmembers, sea-ice melt (SIM: S = 5 and TA = 349 μmol kg^{-1}) and riverine output (RRO: S = 0 and TA = 793 μmol kg^{-1}).

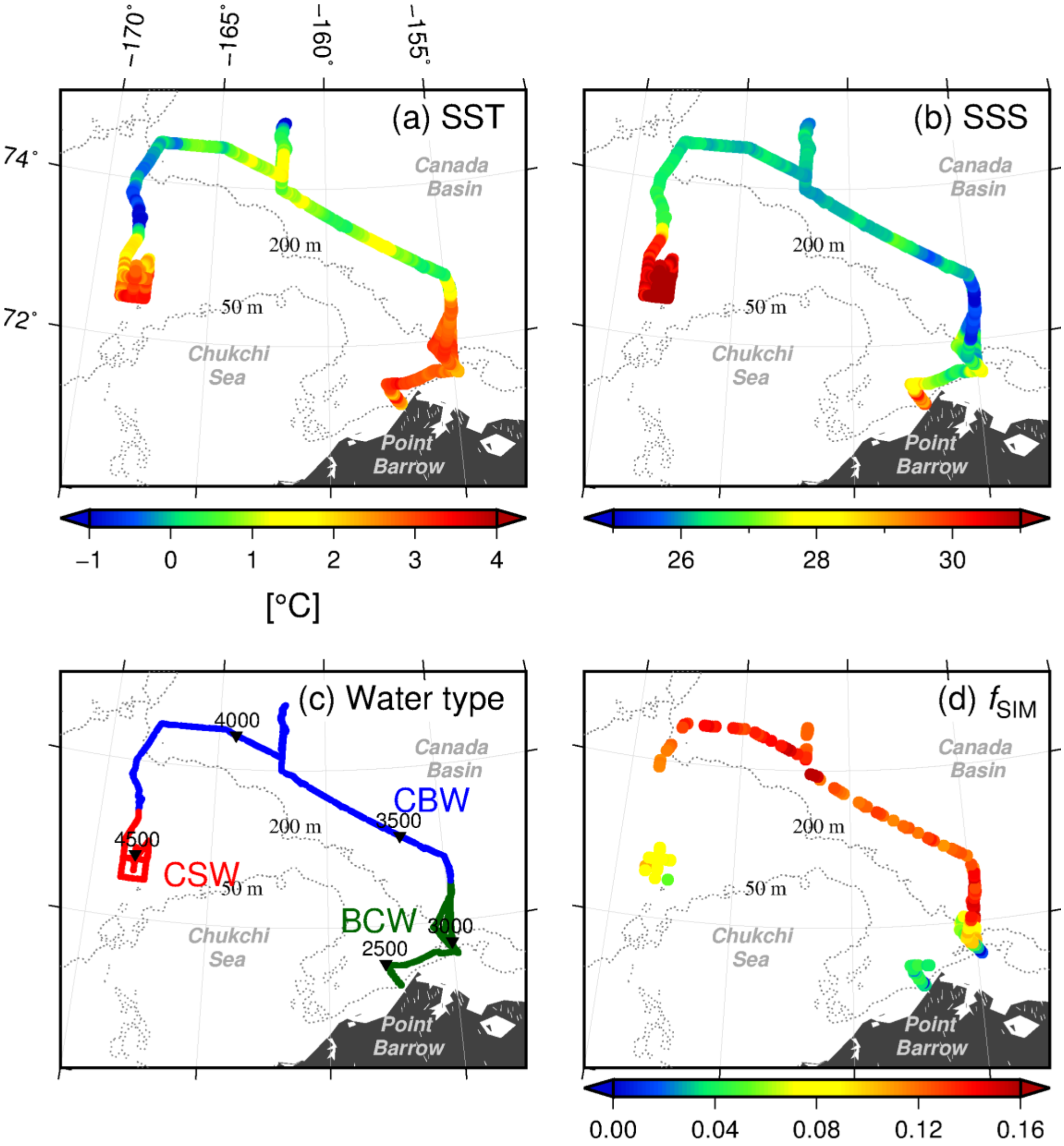
−170°
−165°
−160°
−155°
74°
72°
(a) SST
(b) SSS
(c) Water type
(d) f_{SIM}
Canada Basin
200 m
50 m
Chukchi Sea
Point Barrow
−1
0
1
2
3
4
[°C]
26
28
30
4000
3500
4500
3000
2500
CBW
CSW
BCW
0.00
0.04
0.08
0.12
0.16

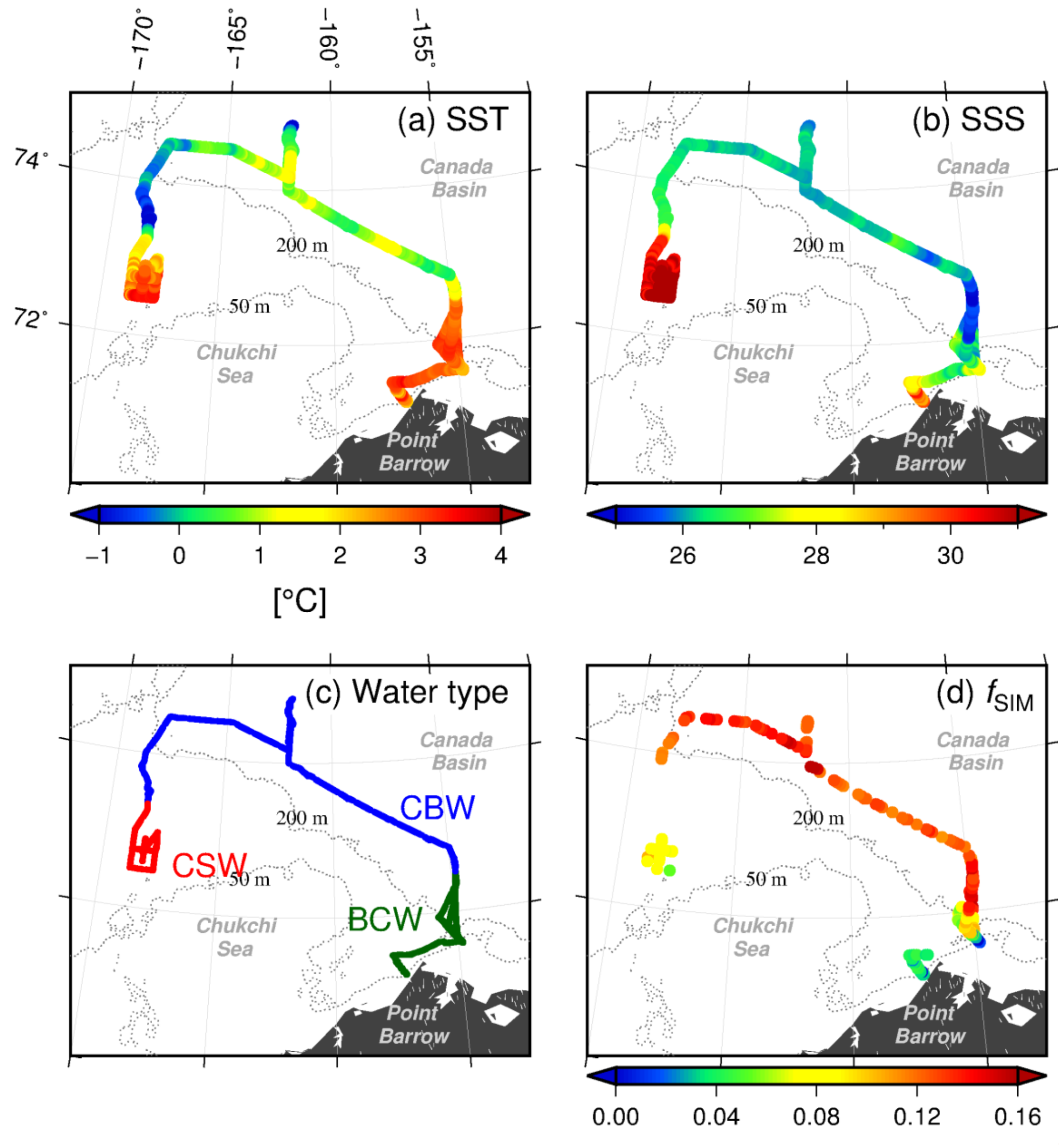

Figure 3: Surface water properties along the track of cruise MR13-06 from 4 to 11 September 2013. (a) Sea surface temperature (SST), (b) sea surface salinity (SSS), (c) BCW (Barrow Coastal Water), CSW (Chukchi Sea Water), and CBW (Canada Basin Water) water type according to SST and SSS. Number on triangles indicates distance sailed from Dutch harbor, Alaska, USA [km], (d) f_{SIM}, (e) f_{RRO}, (f) pCO_2^{sea}, (g) $nDIC_{32}$ = DIC / S * 32; DIC normalized to S =32 and (h) nTA_{32} = TA / S * 32; TA normalized to S =32 . Dotted lines indicate 50 and 200 m isodepths.

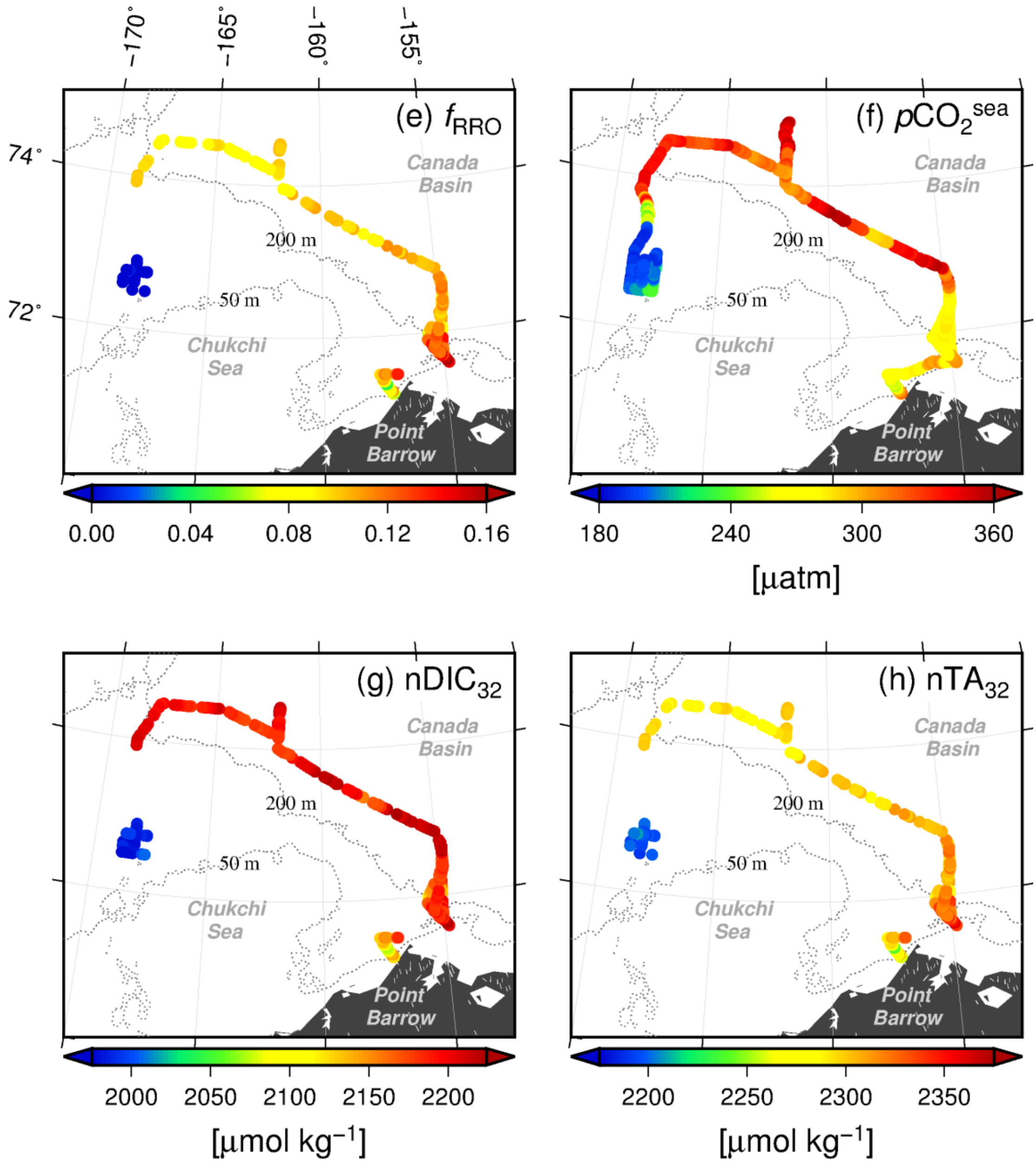

Figure 3 (continued)

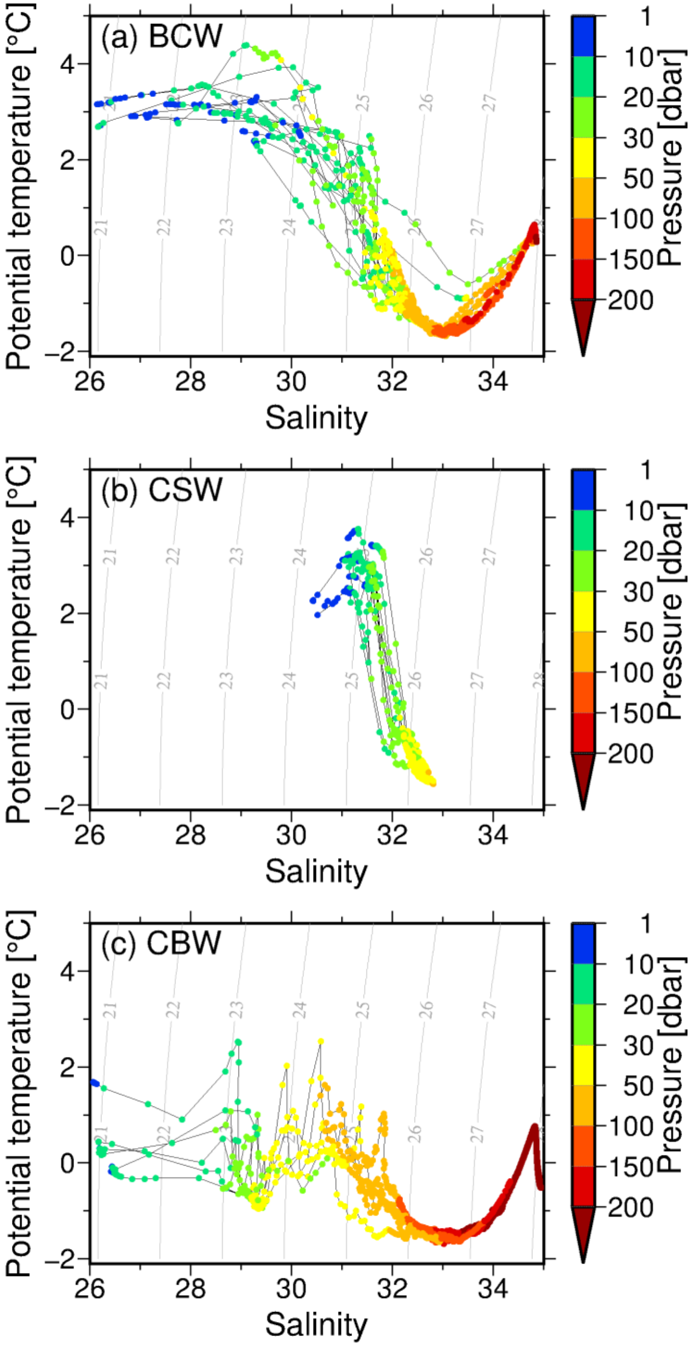

Figure 4: Column salinity and potential temperature in (a) BCW (Barrow Coastal Water), (b) CSW (Chukchi Sea Water), and (c) CBW (Canada Basin Water). Water pressure is indicated by color. Gray contours indicate potential density (σ_θ = {density – 1} × 1000 [kg m^{-3}]).

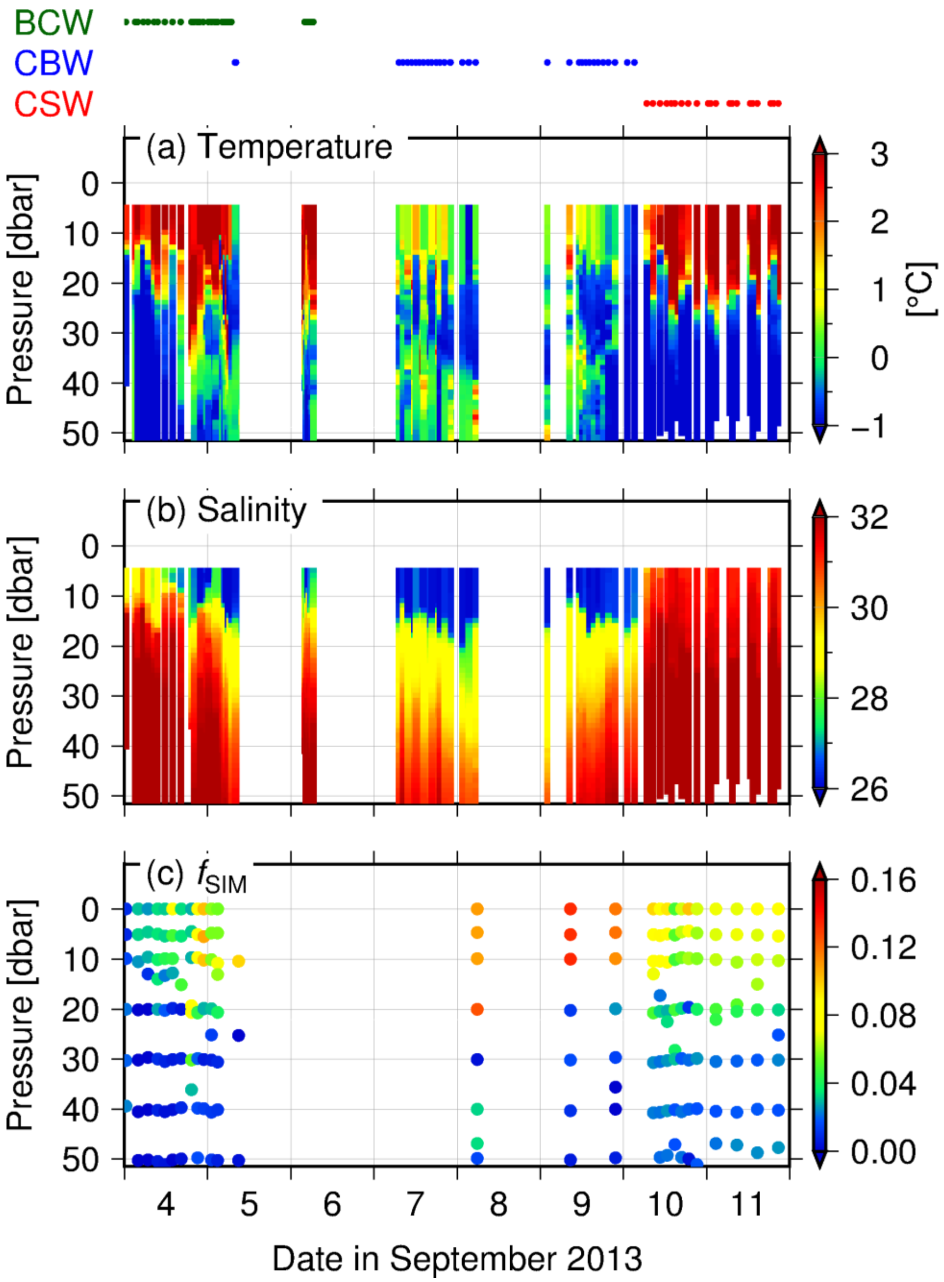
BCW
CBW
CSW
(a) Temperature
Pressure [dbar]
0
10
20
30
40
50
3
2
1
0
−1
[°C]
(b) Salinity
Pressure [dbar]
0
10
20
30
40
50
32
30
28
26
(c) f_{SIM}
Pressure [dbar]
0
10
20
30
40
50
0.16
0.12
0.08
0.04
0.00
4
5
6
7
8
9
10
11
Date in September 2013

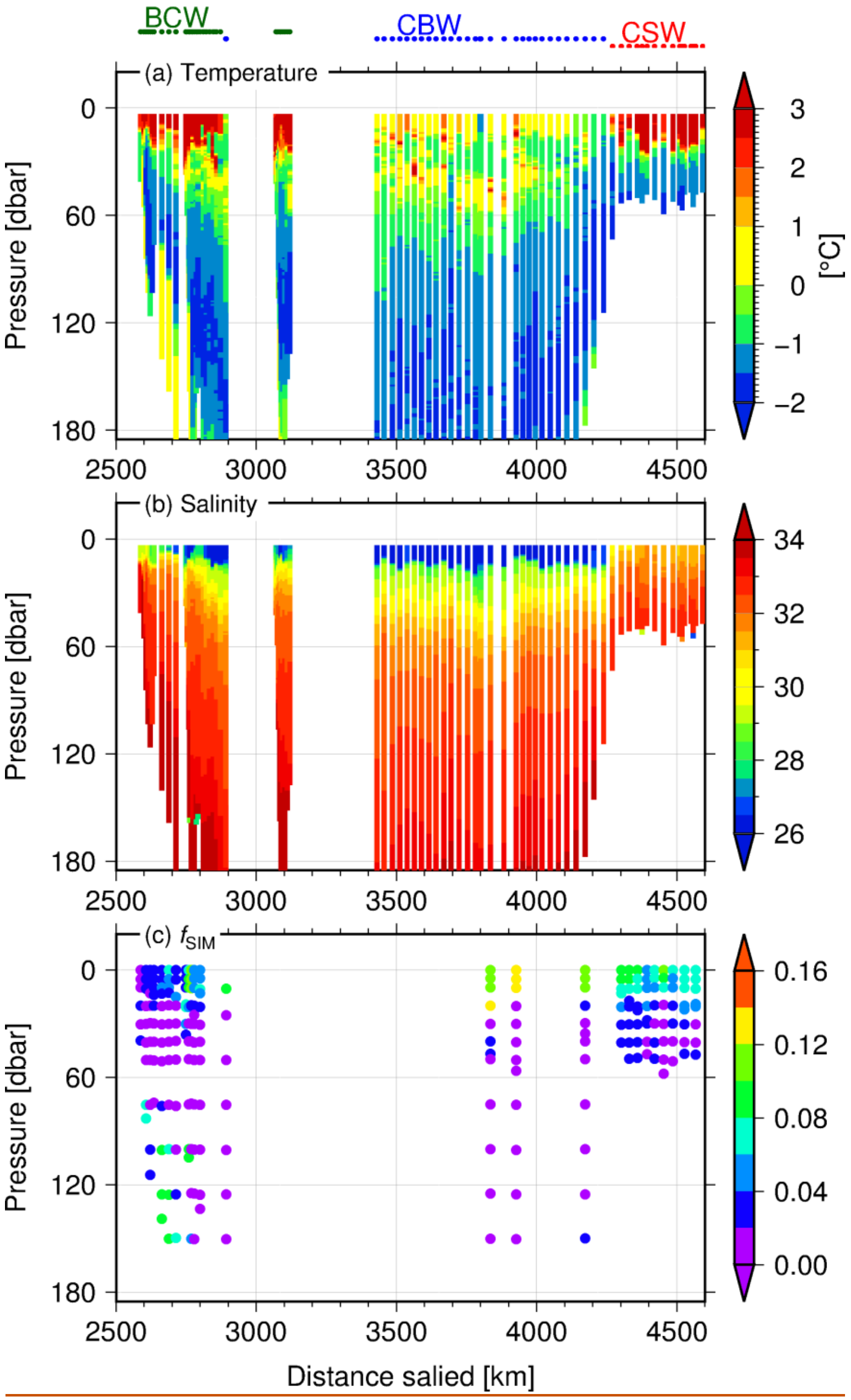

Figure 5: Water ~~C~~column profiles of (a) temperature, (b) salinity, (c) f_{SIM}, (d) f_{RRO}, (e) pCO$_2^{sea}$, and (f) apparent oxygen utilization (AOU) along the cruise track in the period 4–11 September 2013. Data were obtained by CTD and XCTD in (a) and (b), by oxygen sensor SBE43 on CTD in (f), and by discrete bottle samples in (c), (d) and (e). Water types BCW (Barrow Coastal Water, CBW (Canada Basin Water), and CSW (Chukchi Sea Water) are indicated at the top of the figure.

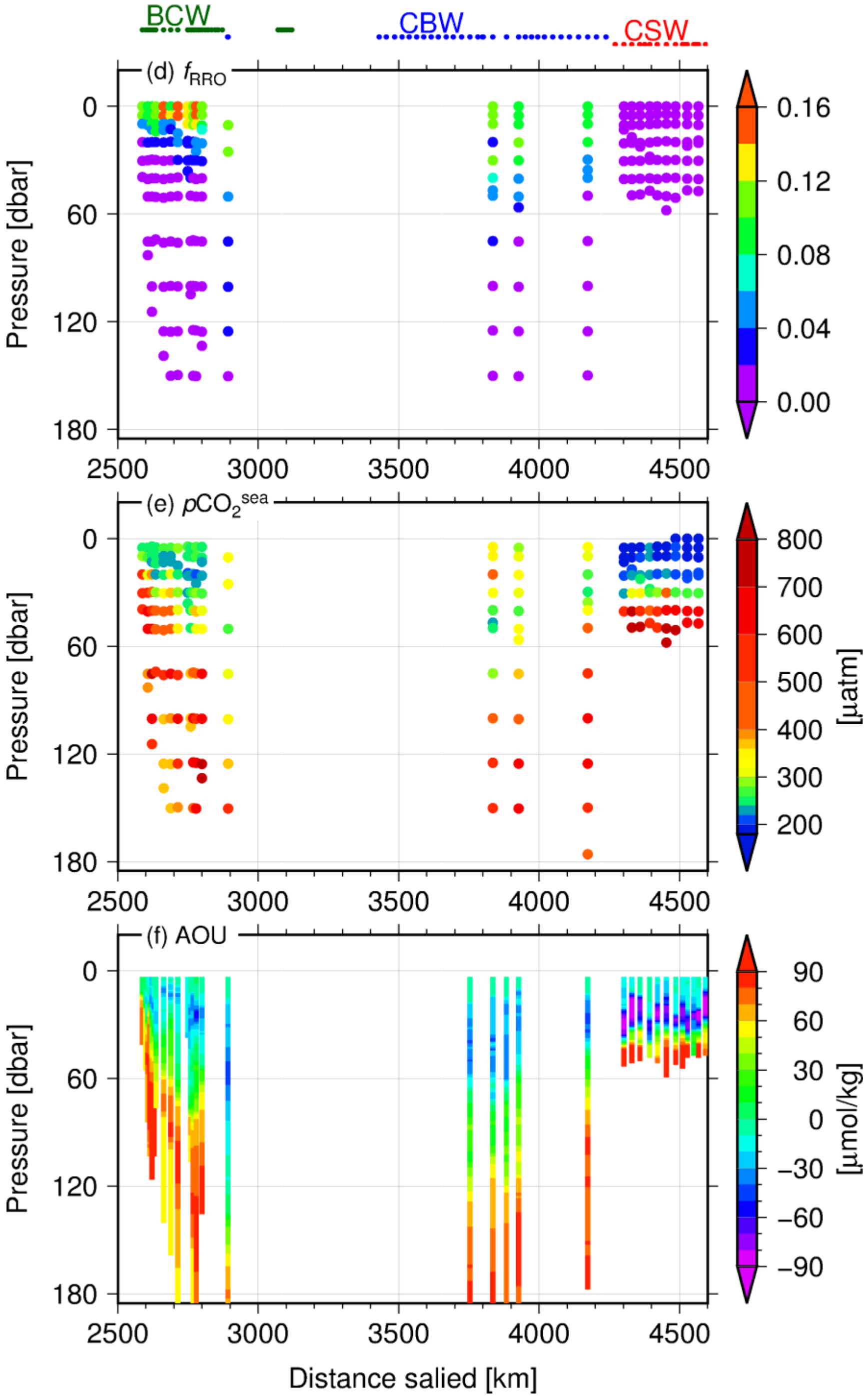
BCW
CBW
CSW
(d) f_{RRO}
(e) $p\mathrm{CO_2}^{sea}$
(f) AOU
Pressure [dbar]
0
60
120
180
2500
3000
3500
4000
4500
0.16
0.12
0.08
0.04
0.00
800
700
600
500
400
300
200
[µatm]
90
60
30
0
−30
−60
−90
[µmol/kg]
Distance salied [km]

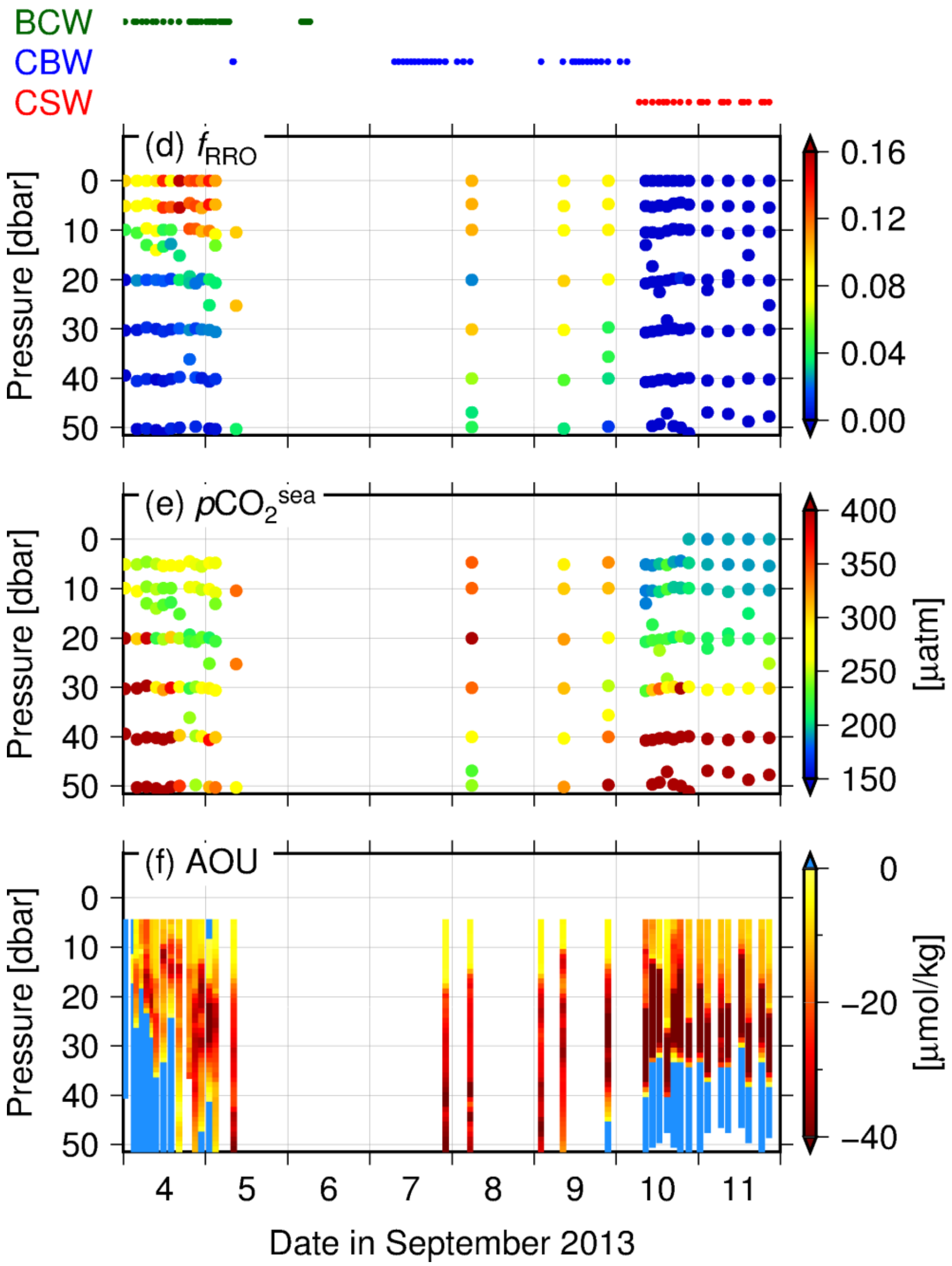

Figure 5 (continued)

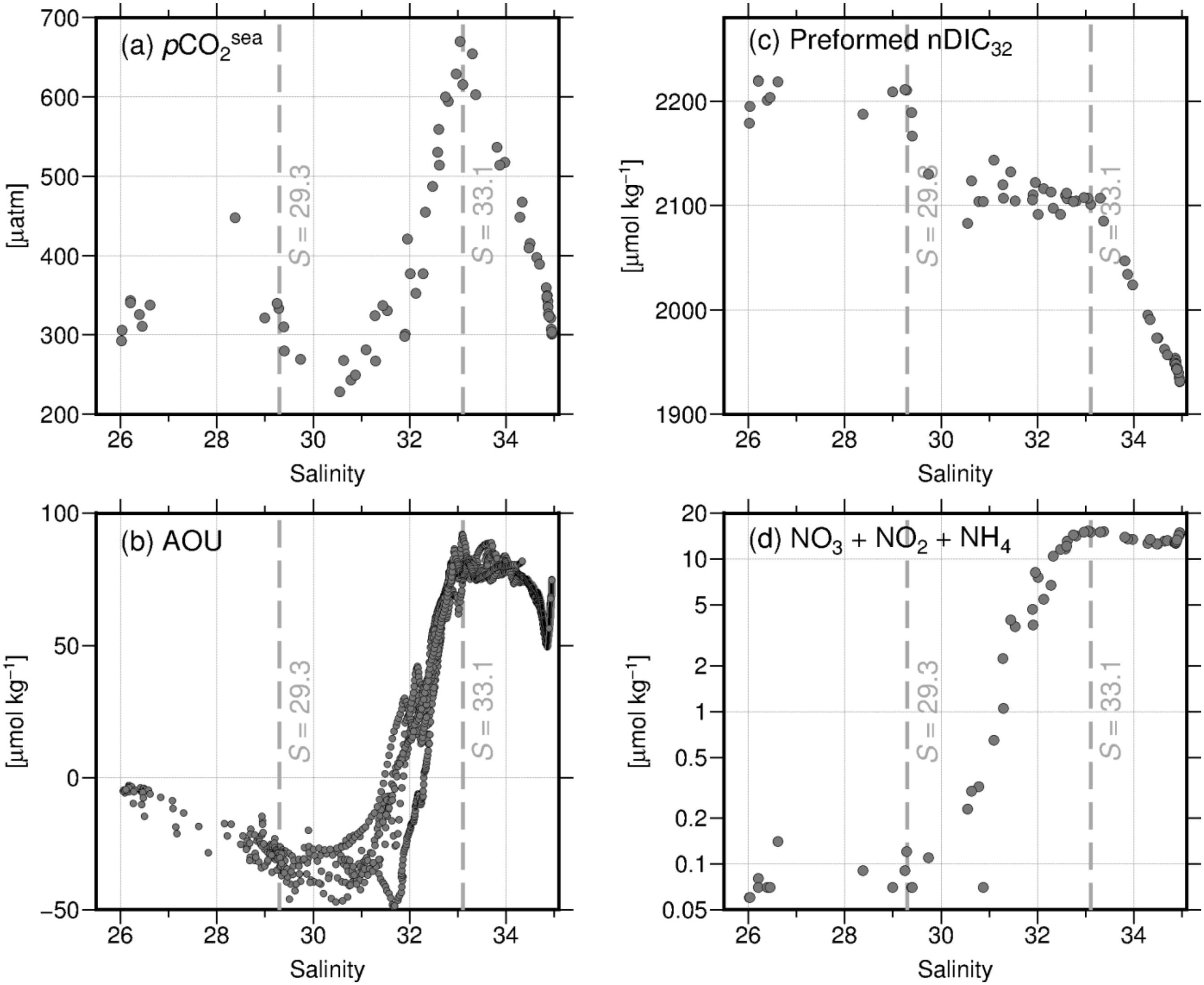

(a) pCO_2^{sea}
[µatm]
700
600
500
400
300
200
S = 29.3
S = 33.1
26
28
30
32
34
Salinity
(c) Preformed $nDIC_{32}$
[µmol kg^{-1}]
2200
2100
2000
1900
S = 29.3
S = 33.1
26
28
30
32
34
Salinity
(b) AOU
[µmol kg^{-1}]
100
50
0
−50
S = 29.3
S = 33.1
26
28
30
32
34
Salinity
(d) $NO_3 + NO_2 + NH_4$
[µmol kg^{-1}]
20
10
5
2
1
0.5
0.2
0.1
0.05
S = 29.3
S = 33.1
26
28
30
32
34
Salinity

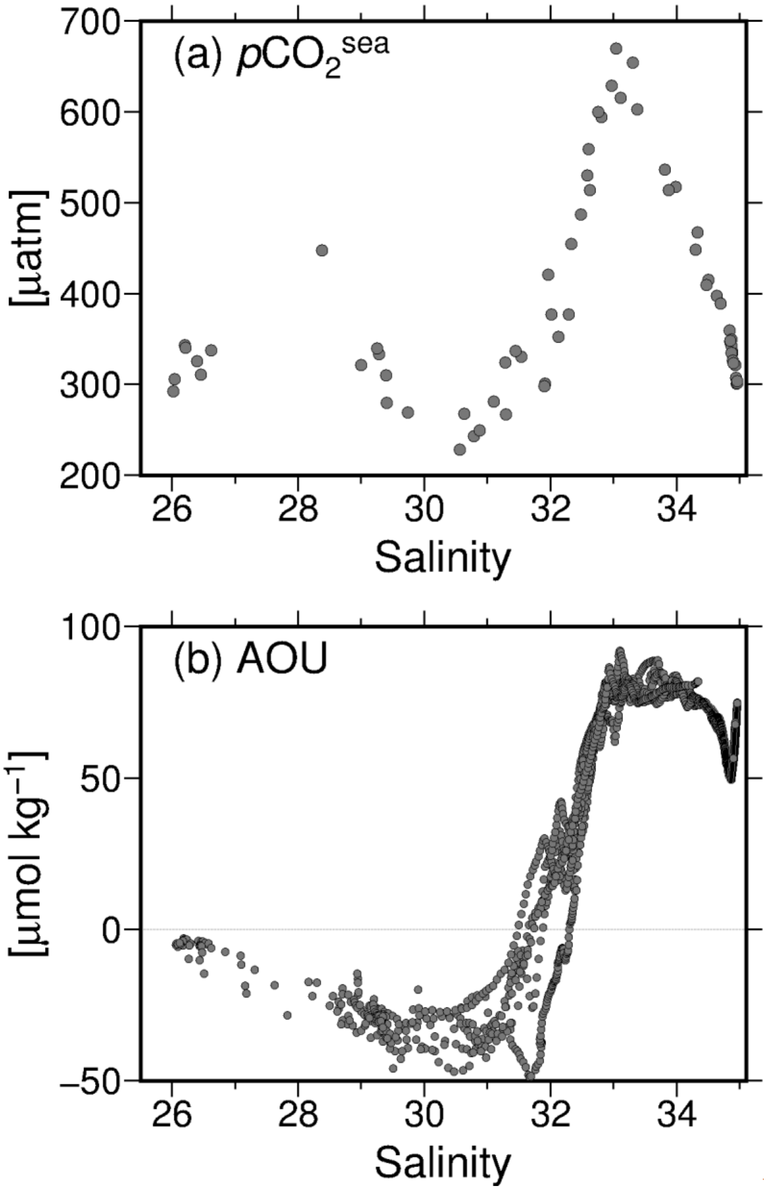

Figure 6: Variation in several parameters of Canada Basin Water against salinity. ~~Canada Basin Water values for (a) salinity and pCO$_2^{sea}$ in discrete bottle samples and (b) salinity and apparent oxygen utilization (AOU) from CTD cast data.~~(a) pCO$_2^{sea}$ in discrete bottle samples, (b) apparent oxygen utilization (AOU) from CTD cast data, (c) preformed nDIC$_{32}$ (= {DIC – AOU * 117 / 170} / S * 32) in discrete bottle samples and dissolved nitrate (NO$_3$ + NO$_2$ + NH$_4$) in logarithmic scale in discrete samples. Salinity of rWML (S = 29.3) and PWW (S = 33.1) were indicated as gray dotted lines.

Table 1: Summary of three water types (BCW, Barrow Coastal Water; CBW, Canada Basin Water; and CSW, Chukchi Sea Water) at the surface in the western Arctic Ocean. All samples were pumped up underway from an intake at ship's bottom. Values are averages for samples collected from 4 to 11 September 2013. N denotes the number of samples. nDIC$_{32}$ and nTA$_{32}$ are DIC and TA normalized to S =32 respectively (nDIC$_{32}$ = DIC / S * 32; nTA$_{32}$ = TA / S * 32). Standard deviation (SD) was listed below each value.

~~Water type~~	~~N~~	~~T [°C]~~	~~S~~	~~DIC [µmol kg^{-1}]~~	~~nDIC$_{32}$ [µmol kg^{-1}]~~	~~TA [µmol kg^{-1}]~~	~~nTA$_{32}$ [µmol kg^{-1}]~~	~~DIC/TA~~	~~pCO$_2^{sea}$ [µatm]~~	~~f_{SIM}~~	~~f_{RRO}~~
~~BCW~~	~~109~~	~~2.88~~	~~27.01~~	~~1827~~	~~2166~~	~~1948~~	~~2309~~	~~0.938~~	~~274~~	~~0.11~~	~~0.08~~
~~CBW~~	~~118~~	~~0.66~~	~~26.19~~	~~1803~~	~~2203~~	~~1882~~	~~2299~~	~~0.958~~	~~332~~	~~0.10~~	~~0.12~~
~~CSW~~	~~54~~	~~3.03~~	~~31.06~~	~~1923~~	~~1982~~	~~2131~~	~~2196~~	~~0.903~~	~~198~~	~~−0.01~~	~~0.08~~

Water Type	N	T [°C]	S	DIC [µmol kg^{-1}]	nDIC$_{32}$ [µmol kg^{-1}]	pCO$_2$ [µatm]	TA [µmol kg^{-1}]	nTA$_{32}$ [µmol kg^{-1}]	DIC/TA	f_{RRO}	f_{SIM}
BCW	109	2.88	27.01	1827	2166	274	1948	2309	0.938	0.11	0.08
SD		±0.30	±1.37	±72	±34	±13	±85	±25	±0.006	±0.02	±0.04
CBW	118	0.66	26.19	1803	2203	332	1882	2299	0.958	0.10	0.12
SD		±0.58	±0.24	±19	±16	±19	±16	±9	±0.004	±0.01	±0.01
CSW	54	3.03	31.06	1923	1982	198	2131	2196	0.903	-0.01	0.08
SD		±0.23	±0.19	±13	±6	±19	±12	±3	±0.002	±0.00	±0.01